

Exact solution for the Lindbladian dynamics for the open XX spin chain with boundary dissipation

Kohei Yamanaka¹ and Tomohiro Sasamoto¹

¹*Department of Physics, Tokyo Institute of Technology, Ookayama 2-12-1, Tokyo 152-8551, Japan*
(Dated: April 26, 2021)

We obtain exact formulas for the time-dependence of a few physical observables for the open XX spin chain with Lindbladian dynamics. Our analysis is based on the fact that the Lindblad equation for an arbitrary open quadratic system of N fermions is explicitly solved in terms of diagonalization of a $4N \times 4N$ matrix called structure matrix by following the scheme of the third quantization. We mainly focus on the time-dependence of magnetization and spin current. We observe that the spatio-temporal dependence of magnetization and spin current show the light-cone structure. Moreover, for a fixed site, we observe specific behaviors which are not seen in the closed XX spin chain. Near the center of the chain, these quantities exhibit an exponential approach to the steady state values and the decay time is given by the Liouvillian gap. The contribution of the corresponding state becomes smaller for sites near a boundary, where we observe a plateau regime where magnetization does not change over a duration of time. Using the fact that the time derivative of magnetization is written as a product of the Bessel function and exponential function, we can explain various properties of the plateau regime analytically.

I. INTRODUCTION

Open non-equilibrium systems, connected with external reservoirs, have been one of the most important subjects in non-equilibrium statistical mechanics[1, 2]. They are known to show various interesting behaviors and phenomena, which are not seen in systems in thermal equilibrium. A classical example is the Bernard convection, in which a characteristic spatio-temporal pattern appears when the temperature difference between the top and bottom sides of an intermediate liquid becomes large enough[3–5]. To understand basic properties of non-equilibrium systems, studying simple model systems is useful. In particular, there have been extensive studies on classical one-dimensional models which show nontrivial phenomena like boundary induced phase transition and anomalous transport and at the same time are analytically tractable[6–8].

Recently, due to the development of experimental techniques, non-equilibrium states are realized also in a variety of quantum systems, such as cold atoms[9–12], the optics[13, 14], and the quantum walks[15]. Correspondingly studying non-equilibrium properties of open quantum systems from a theoretical point of view are also becoming more and more important. In addition, for the last few years, connections to studies of topological natures for non-hermitian systems[16–20] are suggested and attract attention, since open quantum systems can be interpreted as non-hermitian systems.

There are a few theoretical frameworks to study the dynamics of open quantum systems. A conventional one is the use of non-equilibrium Green's function (NEGF)[21, 22], which is an extension of the standard Green's function[22, 23] and has been useful to analytically calculate time dependent correlation functions for systems in equilibrium. Recently, the method has been generalized to study systems in which the state evolves from a given initial condition to another[24, 25]. It has been already applied to a few concrete models such as the one-dimensional XY spin chain[26–28]. In this approach, the time evolution is still given by a Hamiltonian, but calculations tend to be rather cumbersome. It has turned out that a description by a quantum master equation (QME)[29–31] is equally effective and useful to study various properties of non-equilibrium systems. There are several versions of the QMEs, such as the Lindblad equation and the Redfield equation. In this paper we employ the description by the Lindblad equation. In many works, the Lindblad equation has been solved numerically. But it is not enough in particular when we want to study non-equilibrium properties of large systems.

As for simple systems, studying these with many degrees of freedom whose dynamics is described by Lindblad equations would be useful. Indeed there have been already many previous works for several one-dimensional systems described by the Lindblad equation. In particular, several exact solutions for nonequilibrium steady states(NESSs) have been obtained by using Matrix Product Ansatz (MPA)[32–40]. As for dynamics, there have been also impressive recent progress for numerical calculations such as the Matrix Product Operator method[41–43], the density matrix renormalization group method[44, 45], and so on. It is equally important to develop analytical techniques to study their dynamics. In particular, analytical solutions for some simple model systems would provide invaluable information for understanding general open quantum systems.

In this paper, we will give an exact solution for the time-dependence of the magnetization and the spin current for the XX spin chain with boundary dissipation described by the Lindblad equation. We will use the fact that an

arbitrary open quadratic system whose dynamics is described by the Lindblad equation admits an application of the third quantization[46]. Although this method has been already known for about ten years and has been applied to several fermionic and bosonic systems[46–52], as far as we know, it has not been fully exploited for obtaining exact formulas for time-dependent physical quantities. In this paper we will show how we can utilize the third quantization to obtain exact time-dependence of physical quantities and provide explicit formulas for a few of them.

In previous works [46, 48–52], solving a Lindblad equation describing the dynamics for open quadratic bosonic/fermionic systems has been shown to reduce to a diagonalization of a $2N \times 2N$ matrix. In this paper, we first show that, in the case of the open XX spin chain, the problem can be further reduced to a diagonalization of an $N \times N$ non-Hermitian matrix and that this non-Hermitian matrix can be diagonalizable. Then we will show that the time-dependence of physical quantities can be studied by solving the continuous-time differential Lyapunov equation[53–55] and that this equation can indeed be solvable. By combining these we can arrive at explicit formulas for the time-dependence for an open quantum system described by the Lindblad equation.

As an example of applications of our formulas, we consider the time-dependence of the magnetization and the spin current from the thermal equilibrium state in high temperature limit $\beta \rightarrow 0$. First, by taking the limit $t \rightarrow \infty$, we obtain the exact solutions for NESS. We will see that our formulas give a generalization of the formulas in a previous study using MPA [33], in which only the case of opposite magnetizations at the boundaries was treated. By the same formulas, we will also analyze behaviors for time-dependent physical observables. By carefully examining the formulas, we observe that the spatio-temporal dependence of the magnetization for the open XX chain using our formulas shows a light-cone structure. A light-cone structure is shown in the quench dynamics or a dynamics starting from the step initial condition, and our study is important to discuss the similarity and difference with the dynamics of the closed XX spin chain[11, 56, 57] and the validity of some approximations in the derivation of the QMEs[31]. Moreover, by examining the formulas at the specific sites, such as a site near a boundary and a site near the center of the chain, we can observe the specific behaviors which can not be observed in the closed XX spin chain. We can analytically show that the magnetization and the spin current at the center of the chain approach the steady state values slowly with oscillations, whereas the magnetization and the spin current on a site near a boundary approach the steady state values with oscillations after finishing the plateau regime where the magnetization does not change over a duration of time. At another bulk site, as a site gets close to the center of the chain, the plateau regime is quickly short by a fluctuation and the convergence to the steady state value is slow. In particular, we discuss several behaviors in detail such as the mechanism of the light-cone structure and the appearance of the plateau regime near boundaries.

The paper is organized as follows. In the following section 2, we shortly explain the general theorems of the third quantization to review the previous studies[46, 50], and we calculate the exact spectrum of the Lindbladian. In section 3, we explain the main results in this paper. These are that: (i) we can calculate the analytical steady state solutions of the magnetization and spin current for open XX spin chain with left-right asymmetric dissipation strength and bath magnetization, and (ii) the exact solutions of the time-dependence of magnetization and spin current are obtained, and these behaviors for the sites near either left or right boundary are different to the ones for bulk sites. We focus on the plateau regime where the magnetization does not change over a duration of time in the behaviors of the time-dependence of the magnetization and the spin current, in particular. In section 4, we summarize this paper, and in appendixes we comment on the more detailed calculations for the physical observables for steady state and the time-derivative of the magnetization on an arbitrary site.

II. SPECTRUM OF THE OPEN XX SPIN CHAIN WITH BOUNDARY DISSIPATION

A. Lindbladian in Liouvillian-Fock space

We consider the following Hamiltonian of XX spin chain,

$$H = J \sum_{k=1}^{N-1} (\sigma_k^x \sigma_{k+1}^x + \sigma_k^y \sigma_{k+1}^y) - B \sum_{k=1}^N \sigma_k^z, \quad (1)$$

where $\sigma_k^{x,y,z}$ are the Pauli operators, J is the coupling constant between a site and nearest-neighbor sites, and B is denoted as the magnetic field. The Lindblad equation [30] is denoted as

$$\frac{d}{dt}\rho(t) = \mathcal{L}\rho(t) \equiv -i[H, \rho(t)] + \sum_{\mu} L_{\mu}\rho(t)L_{\mu}^{\dagger} - \frac{1}{2}\{L_{\mu}^{\dagger}L_{\mu}, \rho(t)\}, \quad (2)$$

where $\rho(t)$ is the density operator and Lindblad dissipative operators are defined as

$$L_1 = \sqrt{\varepsilon_L \frac{1 + \mu_L}{2}} \sigma_1^+, \quad L_3 = \sqrt{\varepsilon_R \frac{1 + \mu_R}{2}} \sigma_N^+, \quad (3)$$

$$L_2 = \sqrt{\varepsilon_R \frac{1 - \mu_L}{2}} \sigma_1^-, \quad L_4 = \sqrt{\varepsilon_R \frac{1 - \mu_R}{2}} \sigma_N^-, \quad (4)$$

where $\sigma^\pm = (\sigma^x \pm i\sigma^y)/2$, $\varepsilon_{L/R}$ are dissipative strength between system and each reservoirs, and $\mu_{L/R}$ are the magnetization on each reservoirs. We can explain the interpretation of these parameters and the forms of the operators (3,4) when we derive the Lindblad equation from the dynamics of the total system including the reservoirs [58, 59]. The Lindblad operators L_1, L_2 (3,4) play the roles of entry and exclusion of the up-spin between left boundary and left end, and L_3, L_4 (3,4) play the roles of entry and exclusion for the up-spin between right boundary and right end. These parameters $\varepsilon_{L/R}, \mu_{L/R}$ are related to the coupling strength in each boundary and the reservoir's chemical potential.

Then, we introduce the Majorana fermion operators w_j , $j = 1, 2, \dots, 2N$ satisfying the anticommutation relations $\{w_j, w_k\} = 2\delta_{j,k}$. The XX spin chain is equivalent to the one-dimensional free Majorana fermion model using the inverse of the Jordan-Wigner transformation $\sigma \rightarrow w$. These operators w_j are related to Pauli operators σ_m as the following Jordan-Wigner transformation [46],

$$w_{2k-1} = \sigma_k^x \prod_{n < k} \sigma_n^z, \quad w_{2k} = \sigma_k^y \prod_{n < k} \sigma_n^z, \quad 1 \leq k \leq N. \quad (5)$$

This Hamiltonian in (1) and Lindblad dissipative operators in (3,4) are rewritten in terms of the Majorana fermion operators w_j as

$$H = -iJ \sum_{k=1}^{N-1} (w_{2k} w_{2k+1} - w_{2k-1} w_{2k+2}) + iB \sum_{k=1}^N w_{2k-1} w_{2k}, \quad (6)$$

and as

$$L_1 = \sqrt{\varepsilon_L \frac{1 + \mu_L}{2}} \frac{w_1 + iw_2}{2}, \quad L_3 = \sqrt{\varepsilon_R \frac{1 + \mu_R}{2}} \frac{w_{2N-1} + iw_{2N}}{2} \Omega, \quad (7)$$

$$L_2 = \sqrt{\varepsilon_R \frac{1 - \mu_L}{2}} \frac{w_1 - iw_2}{2}, \quad L_4 = \sqrt{\varepsilon_R \frac{1 - \mu_R}{2}} \frac{w_{2N-1} - iw_{2N}}{2} \Omega, \quad (8)$$

respectively. Here, $\Omega := (-1)^N \prod_{l=1}^{2N} w_l$ is a Casimir operator which commutes with all the elements of the Clifford algebra generated by Majorana operators w_j , and satisfies $\Omega \Omega^\dagger = \Omega^\dagger \Omega = 1$.

Throughout this paper, $\underline{x} = (x_1, x_2, \dots)^T$ will designate a vector (column) of appropriate scalar valued or operator valued symbols x_k . Then, the Hamiltonian and the Lindblad dissipative operators (6-8) can be expressed in a form of a quadratic form and linear forms respectively as

$$H = \sum_{j,k=1}^{2N} w_j H_{j,k} w_k = \underline{w} \cdot \mathbf{H} \underline{w}, \quad (9)$$

$$L_\mu = \sum_{j=1}^{2N} l_{\mu,j} w_j = \underline{l}_\mu \cdot \underline{w}, \quad (10)$$

where $\underline{A} \cdot \underline{B}$ is the inner product between the vectors \underline{A} and \underline{B} , and $2N \times 2N$ matrix \mathbf{H} can be chosen to be an antisymmetric matrix $\mathbf{H}^T = -\mathbf{H}$. From Lindblad dissipative operators, the matrix \mathbf{M} is defined as

$$M_{jk} = \sum_{\mu} l_{\mu,j} l_{\mu,k}^*, \quad (11)$$

which is a Hermitian matrix, and \mathbf{M}_R and \mathbf{M}_I are real and imaginary part of the matrix \mathbf{M} , respectively.

A fundamental concept of the third quantization[46] is the Fock structure on 4^N -dimensional Liouville space of operators \mathcal{K} , called the operator space. This space is created as the Hilbert space of density operators with the definition of an inner product $\langle A|B \rangle = 4^{-N} \text{tr}(A^\dagger B)$ where A, B are operators. We use Dirac bra-ket notation for the operator space \mathcal{K} . This means replacing the relation between operators and states over physical Hilbert space to the one between maps and operators over the operator space. Then, symbols with a hat shall designate linear maps over

the operator space \mathcal{K} , and we note the difference between an operator X over the physical Hilbert space and a map \hat{X} over operator space \mathcal{K} . By this transformation, the Lindblad equation (2) is rewritten as

$$\frac{d}{dt} |\rho(t)\rangle = \hat{\mathcal{L}} |\rho(t)\rangle. \quad (12)$$

The Lindblad map $\hat{\mathcal{L}}$ is written in terms of the self-adjoint Hermitian Majorana fermion maps $\hat{a}_{\mu,r}$ [46] satisfying $\{\hat{a}_{\mu,r}, \hat{a}_{\nu,s}\} = \delta_{\mu,\nu} \delta_{r,s}$, and this map takes a quadratic form with the identity map term $\mathbb{1}$ as

$$\hat{\mathcal{L}} = \underline{\hat{a}} \cdot \mathbf{A} \underline{\hat{a}} - A_0 \mathbb{1}, \quad (13)$$

where a matrix \mathbf{A} is called the structure matrix

$$\mathbf{A} = \begin{pmatrix} -2i\mathbf{H} + i\mathbf{M}_I & i\mathbf{M} \\ -i\mathbf{M}^T & -2i\mathbf{H} - i\mathbf{M}_I \end{pmatrix}, \quad (14)$$

and the coefficient of identity term A_0 is equal to the trace of the matrix \mathbf{M} .

The Lindblad map conserves its parity. The operator space \mathcal{K} can be decomposed into a direct sum $\mathcal{K} = \mathcal{K}_+ \oplus \mathcal{K}_-$ which are defined as $\mathcal{K}_{\pm} = \frac{1 \pm \exp(i\pi \sum_k (\frac{1}{2} - i\hat{a}_{1,k}\hat{a}_{2,k}))}{2} \mathcal{K}$. Then, the parity of the Lindblad map in the operator space \mathcal{K} corresponds to that of total number of Majorana operator w_j in physical Hilbert space \mathcal{H} . In this paper, we consider only the product of an even number of Majorana fermion operator w_j , which is enough to calculate usual physical observables, for example magnetization, spin current, energy, and so on. Thus, we can restrict our attention to the subspace \mathcal{K}_+ . If the structure matrix \mathbf{A} is written as the Jordan canonical form, the Lindblad map $\hat{\mathcal{L}}$ becomes the almost-diagonal maps. Moreover, we obtain the exact solution of the time-dependence of physical observables whose dynamics are described by the Lindblad equation.

B. Exact Spectrum of Lindbladian

As shown in [49], the structure matrix \mathbf{A} is unitary equivalent to a following block-triangular matrix,

$$\tilde{\mathbf{A}} = \mathbf{U} \mathbf{A} \mathbf{U}^\dagger = \begin{pmatrix} -\mathbf{X}^T & 2i\mathbf{M}_I \\ 0 & \mathbf{X} \end{pmatrix}, \quad (15)$$

where $\mathbf{X} = -2i\mathbf{H} + \mathbf{M}_R$ is a real matrix, and the matrix \mathbf{U} is trivially the $4N \times 4N$ permutation matrix which corresponds to the cyclic permutation of Pauli operators ($\sigma^x \rightarrow \sigma^y, \sigma^y \rightarrow \sigma^z, \sigma^z \rightarrow \sigma^x$). Also, as shown in [49], if the matrix \mathbf{X} is diagonalizable, the structure matrix is diagonalizable. Thus, we consider only the eigensystem of a $2N \times 2N$ matrix \mathbf{X} . Moreover, we show that we can decompose the matrix \mathbf{X} into $N \times N$ matrices for the open XX spin chain with boundary dissipation, which we are working on.

Lemma 1. Using a unitary matrix \mathbf{S} , the matrix \mathbf{X} is unitarily equivalent to a block-diagonal matrix

$$\begin{aligned} \tilde{\mathbf{X}} &= \mathbf{S} \mathbf{X} \mathbf{S}^\dagger \\ &= \begin{pmatrix} i\Xi & 0 \\ 0 & -i\Xi^\dagger \end{pmatrix}, \end{aligned} \quad (16)$$

where Ξ is an $N \times N$ matrix.

We can show this lemma easily. First, the matrix \mathbf{X} is rewritten by using the Kronecker product

$$\mathbf{X} = -i \begin{pmatrix} -B & -J & & & \\ -J & -B & & & \\ & & \ddots & & \\ & & & -B & -J \\ & & & -J & -B \end{pmatrix} \otimes \sigma^y + \begin{pmatrix} \frac{\varepsilon_L}{4} & & & & \\ & 0 & & & \\ & & \ddots & & \\ & & & 0 & \\ & & & & \frac{\varepsilon_R}{4} \end{pmatrix} \otimes \mathbb{1}_2. \quad (17)$$

Then, we introduce the following permutation,

$$\kappa \mapsto \left\{ \begin{array}{cccccc} 1, & 2, & \cdots, & N, & N+1, & \cdots, & 2N-1, & 2N \\ 1, & 3, & \cdots, & 2N-1, & 2, & 4, & \cdots, & 2N \end{array} \right\}. \quad (18)$$

The $2N \times 2N$ permutation matrices which correspond to the above permutation and the cyclic permutation of Pauli operators are defined to be $\mathbf{\Pi}_\kappa$ and $\tilde{\mathbf{U}}$, and the unitary matrix \mathbf{S} is denoted as $\mathbf{S} = \tilde{\mathbf{U}}\mathbf{\Pi}_\kappa$. The matrix \mathbf{X} is decomposed into the form of a block matrix as

$$\tilde{\mathbf{X}} = \mathbf{S}\mathbf{X}\mathbf{S}^\dagger = \begin{pmatrix} i\mathbf{\Xi} & 0 \\ 0 & -i\mathbf{\Xi}^\dagger \end{pmatrix}, \quad (19)$$

where the matrix $\mathbf{\Xi}$ is non-Hermitian matrix

$$\mathbf{\Xi} = \begin{pmatrix} B - i\frac{\varepsilon_L}{4} & J & & & \\ J & B & & & \\ & & \ddots & & \\ & & & B & J \\ & & & J & B - i\frac{\varepsilon_R}{4} \end{pmatrix}. \quad (20)$$

Also, we can decompose the characteristic polynomial of the matrix \mathbf{X} into two characteristic polynomials of the matrix $\mathbf{\Xi}$, since the matrix $\tilde{\mathbf{X}}$ is block-diagonalizable.

Corollary 1. The characteristic polynomial of the matrix \mathbf{X} is decomposed into two characteristic polynomials of the matrix $\mathbf{\Xi}$

$$p_{\mathbf{X}}(\lambda) = p_{\mathbf{\Xi}}(-i\lambda)p_{\mathbf{\Xi}}^*(-i\lambda^*), \quad (21)$$

where $p_{\mathbf{X}}(\lambda) := \det(\mathbf{X} - \lambda\mathbf{1}_{2N})$, and $p_{\mathbf{\Xi}}(\lambda) := \det(\mathbf{\Xi} - \lambda\mathbf{1}_N)$.

Therefore, all the eigenvalues of the open XX spin chain are constructed by the eigenvalues of the $N \times N$ matrix $\mathbf{\Xi}$. Moreover, the matrix $\mathbf{\Xi}$ is a tri-diagonal matrix and we can obtain the eigenvalues and eigenvectors of the matrix $\mathbf{\Xi}$ [28, 60, 61]. Consider the eigenvalue problem $\mathbf{\Xi}\underline{q} = \lambda\underline{q}$ where the k -th ($1 \leq k \leq N$) eigenvector $\underline{q}^{(k)} = (q_1^{(k)}, q_2^{(k)}, \dots, q_N^{(k)})^T$. The r -th ($1 \leq r \leq N$) component of this eigenvector $q^{(k)}$ can be viewed as the r -th term of an infinite sequence $q^{(k)} = \{q_i^{(k)}\}_{i=0}^\infty$. Then, we obtain the eigenvalue and the component of the eigenvector [60]

$$\lambda^{(k)} = B + 2J \cos \theta_k, \quad (22)$$

and

$$q_j^{(k)} = \frac{q_1}{\sin \theta_k} \left[\sin j\theta_k + i\frac{\varepsilon_L}{4J} \sin(j-1)\theta_k \right], \quad (23)$$

where the parameter θ_k is determined by the following condition,

$$\left\{ 2 \cos \theta_k + i \left(\frac{\varepsilon_L}{4J} + \frac{\varepsilon_R}{4J} \right) \right\} \sin N\theta_k - \left(1 + \frac{\varepsilon_L}{4J} \frac{\varepsilon_R}{4J} \right) \sin(N-1)\theta_k = 0. \quad (24)$$

The distribution of the eigenvalues of the matrix $\mathbf{\Xi}$ has special eigenvalues which has larger imaginary part than the other's one in Fig.1, when boundary dissipative strength $\varepsilon_{L/R}$ are larger than $4J$.

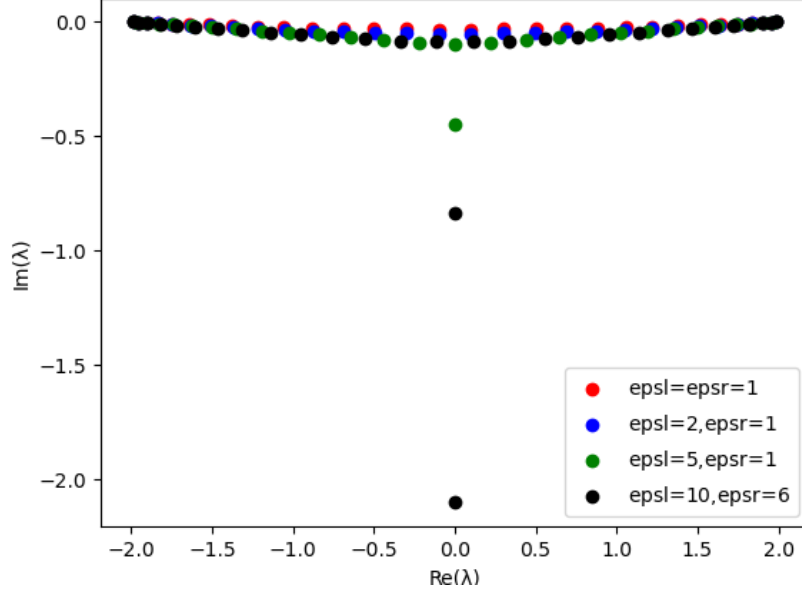


FIG. 1. eigenvalue distribution of matrix Ξ . Other parameters set $N = 30$, $J = 1.0$, $B = 0.0$, and $\mu_L = -\mu_R = 1.0$.

Using the knowledge of the recurrence relation for the matrix Ξ , we obtain the characteristic equation of the matrix Ξ as

$$\beta^{N+1} - \alpha^{N+1} + i \left(\frac{\varepsilon_L}{4J} + \frac{\varepsilon_R}{4J} \right) (\beta^N - \alpha^N) - \frac{\varepsilon_L}{4J} \frac{\varepsilon_R}{4J} (\beta^{N-1} - \alpha^{N-1}) = 0, \quad (25)$$

where $\alpha + \beta = \frac{\lambda - B}{J}$ and $\alpha\beta = 1$. Therefore, if we can solve the equation (25), we obtain the eigenvalue $\lambda = B + J(\beta + \beta^{-1})$. Also, the characteristic equation (25) can be obtained from (24) by $\beta \equiv e^{i\theta_k}$. As shown in [28], the solutions of the above equation are separated by the magnitude of parameter β in long chain limit ($N \rightarrow \infty$). If we consider the solutions which satisfy $|\beta| > 1$, the equation (25) becomes

$$\beta^2 + i \left(\frac{\varepsilon_L}{4J} + \frac{\varepsilon_R}{4J} \right) \beta - \frac{\varepsilon_L}{4J} \frac{\varepsilon_R}{4J} = 0. \quad (26)$$

The solutions of this equation (26) are $\beta = -i \frac{\varepsilon_L}{4J}, -i \frac{\varepsilon_R}{4J}$. These solutions exist only when $\varepsilon_{L/R} > 4J$. In a similar process, the solutions of equation (25) which satisfy $|\beta| < 1$ are $\beta = \frac{4iJ}{\varepsilon_L}, \frac{4iJ}{\varepsilon_R}$. Last, the solution of equation (25) which satisfies $|\beta| = 1$ is $\beta = e^{i\theta}, \theta \in \mathbb{R}$. We call the eigenvalues without imaginary part $\text{Im}(\lambda) = 0$ normal eigenvalue (NE) expressed as $\lambda = B + 2J \cos \theta$ and the eigenvalues with imaginary part $\text{Im}(\lambda) \neq 0$ special eigenvalue (SE) expressed as

$$\lambda = B - iJ \left(\frac{\varepsilon_L}{4J} - \frac{4J}{\varepsilon_L} \right), B - iJ \left(\frac{\varepsilon_R}{4J} - \frac{4J}{\varepsilon_R} \right). \quad (27)$$

Since the matrix Ξ is a complex symmetric matrix, we can diagonalize it by using a complex orthogonal matrix \mathbf{Q} as

$$\Xi = \mathbf{Q} \mathbf{D} \mathbf{Q}^T, \quad \mathbf{D} = \text{diag}[\lambda^{(1)}, \lambda^{(2)}, \dots, \lambda^{(N)}], \quad \mathbf{Q} = \left[\frac{q^{(1)}}{\mathcal{N}_1}, \frac{q^{(2)}}{\mathcal{N}_2}, \dots, \frac{q^{(N)}}{\mathcal{N}_N} \right], \quad (28)$$

where \mathcal{N}_k is the normalization factor of the k -th eigenvector, and is defined as $\mathcal{N}_k \equiv \underline{q}^{(k)} \cdot \underline{q}^{(k)}$. We define $\underline{Q}^{(k)} = \frac{q^{(k)}}{\mathcal{N}_k}$. Then, by Lemma 1. and this diagonalization, the matrix \mathbf{X} is diagonalizable as follows,

$$\mathbf{X} = \mathbf{S}^\dagger \begin{pmatrix} \mathbf{Q} & 0 \\ 0 & \mathbf{Q} \end{pmatrix} \begin{pmatrix} i\mathbf{D} & 0 \\ 0 & -i\mathbf{D}^\dagger \end{pmatrix} \begin{pmatrix} \mathbf{Q}^T & 0 \\ 0 & \mathbf{Q}^\dagger \end{pmatrix} \mathbf{S}. \quad (29)$$

Also, the matrix \mathbf{X} can be rewritten in a Jordan canonical form,

$$\mathbf{X} = \mathbf{P} \mathbf{\Delta} \mathbf{P}^{-1}, \quad (30)$$

where \mathbf{P} is a non-singular matrix, and $\mathbf{\Delta}$ is a Jordan canonical form. Let any Jordan cell size be bigger than 1, and the component of the matrix \mathbf{P} be the generalized eigenvectors of the matrix \mathbf{X} . Thus, if and only if the matrix

\mathbf{X} is diagonalizable, we can consider that these representation are the same. Then, by using (29,30), we obtain the non-singular matrix \mathbf{P} and its inverse matrix \mathbf{P}^{-1} as the follows,

$$\mathbf{P} = \mathbf{S}^\dagger \begin{pmatrix} \mathbf{Q} & 0 \\ 0 & \bar{\mathbf{Q}} \end{pmatrix}, \quad \mathbf{P}^{-1} = \begin{pmatrix} \mathbf{Q}^\top & 0 \\ 0 & \mathbf{Q}^\dagger \end{pmatrix} \mathbf{S}. \quad (31)$$

III. EXACT SOLUTIONS FOR TIME-DEPENDENCE OF PHYSICAL OBSERVABLES

A. Exact formulas for magnetization and current

We consider the time-dependence of quadratic physical observables in terms of Majorana fermion operators. The physical observables $X(t)$ at time t is defined in Schrödinger picture as $X(t) = \text{tr}(X\rho(t))$ [46, 48, 49]. Since the Lindbladian in Hilbert space is difficult to study analytically, we consider the Heisenberg picture in Liouville-Fock space [62, 63]. We can define a quadratic physical observable as following,

$$C_{j,k}(t) = \text{tr}(w_j w_k \rho(t)). \quad (32)$$

Then, since the diagonal terms in $C_{j,k}(t)$ are time-invariant $C_{j,j}(t) = \text{tr}(\rho(t)) = \text{tr}(\rho(0))$, we define the correlation matrix $\tilde{\mathbf{C}}(t) = \left\{ \tilde{C}_{j,k}(t) \right\}_{1 \leq j,k \leq N}$ by

$$\tilde{C}_{j,k}(t) = \text{tr}(w_j w_k \rho(t)) - \delta_{j,k} = 2 \langle 1 | \hat{a}_{1,j}(t) \hat{a}_{1,k}(t) | \rho_0 \rangle - \delta_{j,k}, \quad (33)$$

where the super-Heisenberg picture is defined by $\hat{a}_k(t) := e^{-t\hat{\mathcal{L}}} \hat{a}_k e^{t\hat{\mathcal{L}}}$. Using the Lindbladian map $\hat{\mathcal{L}}$ (13), we can obtain the equation of motion for Majorana map as follows,

$$\frac{d\hat{\mathbf{a}}(t)}{dt} = 2\mathbf{A}\hat{\mathbf{a}}(t). \quad (34)$$

In terms of $\tilde{C}_{j,k}(t)$, the magnetization $m_k^z(t)$ on site k and the spin current $j_{k,k+1}(t)$ between sites k and $k+1$ can be written by using (5) as follows,

$$m_k^z(t) = \langle \sigma_k^z \rangle(t) = -i\tilde{C}_{2k-1,2k}(t), \quad (35)$$

$$j_{k,k+1}(t) = \langle 2J(\sigma_k^x \sigma_{k+1}^y - \sigma_k^y \sigma_{k+1}^x) \rangle(t) = -2Ji\tilde{C}_{2k-1,2k+1}(t) - 2Ji\tilde{C}_{2k,2k+2}(t). \quad (36)$$

The time-dependence of correlation matrix $\tilde{\mathbf{C}}(t)$ satisfies the following differential equation[62, 63],

$$\frac{d\tilde{\mathbf{C}}(t)}{dt} = -2 \left\{ \mathbf{X}^\top \tilde{\mathbf{C}}(t) + \tilde{\mathbf{C}}(t) \mathbf{X} \right\} - 4i\mathbf{M}_I. \quad (37)$$

Since the components of the matrix $\tilde{\mathbf{C}}(t)$ correspond to the physical observables as (35,36), obtaining the exact solution $\tilde{\mathbf{C}}(t)$ (33) is equivalent to obtain the time-dependence of the physical observables. In some papers[62–65], this equation (37) can be solved numerically or can be only examined the steady state ($\frac{d\tilde{\mathbf{C}}(t)}{dt} = 0$), but the fact that this equation(37) is solvable had been known in a different field, such as the control theory[66, 67] and stability analysis[68]. By using the spectrum of the matrix Ξ (20) and the papers[53–55] in the context of variation of constants, we can solve this equation and obtain the time-dependence of the physical observables analytically for the first time.

As shown in [53–55], the time-dependence of correlation matrix is

$$\tilde{\mathbf{C}}(t) = e^{-2t\mathbf{X}^\top} \tilde{\mathbf{C}}(0) e^{-2t\mathbf{X}} + \int_0^t e^{-2s\mathbf{X}^\top} (-4i\mathbf{M}_I) e^{-2s\mathbf{X}} ds. \quad (38)$$

For the above formula(38), we can calculate the exact solution for the time-dependence of the correlation matrix $\tilde{\mathbf{C}}(t)$, if the eigenvalues and the (general) eigenvectors of the matrix \mathbf{X} can be exactly calculated and the correlation matrix in the initial time $\tilde{\mathbf{C}}(0)$ can be determined analytically. For the open XX spin chain, we can obtain the eigenvalues and the (general) eigenvectors of the matrix \mathbf{X} can be exactly calculated. Thus, when we choose the correlation matrix in the initial time $\tilde{\mathbf{C}}(0)$ whose components can be determined analytically, we can obtain the exact solution for the time-dependence of the physical observables, and discuss their behaviors.

In this paper, we introduce the time-dependence from one of the simplest initial states satisfying the condition that the correlation matrix in the initial time $\tilde{\mathbf{C}}(0)$ whose components can be determined analytically. We choose the

thermal equilibrium state in the high-temperature limit ($\beta \rightarrow 0$) as the initial state. Then, the correlation matrix $\tilde{\mathbf{C}}(t)$ in (33) at the time $t = 0$ becomes zero $\tilde{\mathbf{C}}_{j,k}(0) = 0$. Thus, the time-dependence of the correlation matrix takes the following form,

$$\tilde{\mathbf{C}}(t) = \int_0^t e^{-2s\mathbf{X}^T} (-4i\mathbf{M}_I) e^{-2s\mathbf{X}} ds. \quad (39)$$

For the open XX spin chain, since the matrix \mathbf{X} is diagonalizable $\mathbf{X} = \mathbf{P}\mathbf{\Delta}\mathbf{P}^{-1}$, the correlation matrix is calculated as

$$\tilde{\mathbf{C}}(t) = \mathbf{P}^{-T} \left(\left(\int_0^t e^{-2s(\beta_i + \beta_j)} ds \right)_{i,j=1,\dots,2N} \odot (\mathbf{P}^T (-4i\mathbf{M}_I) \mathbf{P}) \right) \mathbf{P}^{-1}, \quad (40)$$

where β_j is an eigenvalue of the matrix \mathbf{X} , and we define the Hadamard product as $(\mathbf{A} \odot \mathbf{B})_{i,j} = A_{i,j} B_{i,j}$. Moreover, since the eigenvalues of \mathbf{X} are calculated from the eigenvalues of the matrix $\mathbf{\Xi}$ from the Corollary 1. and the imaginary parts of the eigenvalues of the matrix $\mathbf{\Xi}$ are negative, the real parts of the eigenvalues of the matrix \mathbf{X} are positive $\text{Re}\{\beta_j\} > 0$. Thus, the integral in (40) can be calculated as

$$\int_0^t e^{-2s(\beta_i + \beta_j)} ds = \frac{1 - e^{-2t(\beta_i + \beta_j)}}{2(\beta_i + \beta_j)}. \quad (41)$$

Therefore, we obtain

$$\tilde{\mathbf{C}}(t) = \mathbf{P}^{-T} \left(\left(\frac{1 - e^{-2t(\beta_i + \beta_j)}}{2(\beta_i + \beta_j)} \right)_{i,j=1,\dots,2N} \odot (\mathbf{P}^T (-4i\mathbf{M}_I) \mathbf{P}) \right) \mathbf{P}^{-1}. \quad (42)$$

The main results in this paper are that we obtain the following exact solutions for time-dependence of magnetization in (35) and spin current in (36). The magnetization $m_k^z(t)$ takes the following form,

$$m_k^z(t) = \sum_{l,n=1}^{2N} \frac{e^{-2t(\beta_l + \beta_n)} - 1}{2(\beta_l + \beta_n)} \mathbf{P}_{2k-1,l}^{-T} [\mathbf{P}^T (4\mathbf{M}_I) \mathbf{P}]_{l,n} \mathbf{P}_{n,2k}^{-1}. \quad (43)$$

Substituting imaginary part of dissipative matrix \mathbf{M} , non-singular matrix \mathbf{P} and that inverse matrix \mathbf{P}^{-1} (31) to (43), the magnetization in (35) takes the following spectral decomposition form,

$$m_k^z(t) = \sum_{l,n=1}^N \text{Re} \left[\frac{1 - e^{-2it(\lambda^{(l)} - \lambda^{(n)*})}}{2i(\lambda^{(l)} - \lambda^{(n)*})} Q_k^{(l)} \left\{ \varepsilon_L \mu_L Q_1^{(l)} Q_1^{(n)*} + \varepsilon_R \mu_R Q_N^{(l)} Q_N^{(n)*} \right\} Q_k^{(n)*} \right]. \quad (44)$$

Similarly, spin current between sites k and $k+1$ $j_{k,k+1}(t)$ in (36), and takes the following spectral decomposition form,

$$j_{k,k+1}(t) = 2J \sum_{l,n=1}^N \text{Im} \left[\frac{1 - e^{-2it(\lambda^{(l)} - \lambda^{(n)*})}}{2i(\lambda^{(l)} - \lambda^{(n)*})} Q_k^{(l)} \left\{ \varepsilon_L \mu_L Q_1^{(l)} Q_1^{(n)*} + \varepsilon_R \mu_R Q_N^{(l)} Q_N^{(n)*} \right\} Q_{k+1}^{(n)*} \right]. \quad (45)$$

In (44,45), the eigenvalues $\lambda^{(j)} = -i\beta_j$ and the matrix elements $Q_k^{(j)}$ are defined by using (22-24,28) and the definition of the normalization factor \mathcal{N}_j as

$$\lambda^{(j)} = B + 2J \cos \theta_j, \quad Q_k^{(j)} = \frac{\frac{1}{\sin \theta_j} \left[\sin k\theta_j + i \frac{\varepsilon_L}{4J} \sin((k-1)\theta_j) \right]}{\sqrt{\sum_{k=1}^N \left(\frac{1}{\sin \theta_j} \left[\sin k\theta_j + i \frac{\varepsilon_L}{4J} \sin((k-1)\theta_j) \right] \right)^2}}, \quad (46)$$

where θ_j satisfies the following equation,

$$\left\{ 2 \cos \theta_k + i \left(\frac{\varepsilon_L}{4J} + \frac{\varepsilon_R}{4J} \right) \right\} \sin N\theta_k - \left(1 + \frac{\varepsilon_L}{4J} \frac{\varepsilon_R}{4J} \right) \sin(N-1)\theta_k = 0. \quad (47)$$

B. Physical observables in steady state

Before going to discussions of dynamical behaviors, in this subsection, we consider briefly the physical observables in steady state which is realized in the long time limit. Taking the limit $t \rightarrow \infty$ in (44,45), magnetization and spin current in steady state are expressed as

$$m_k^z = \sum_{l,n=1}^N \text{Re} \left[\frac{1}{2i(\lambda^{(l)} - \lambda^{(n)*})} Q_k^{(l)} \left\{ \varepsilon_L \mu_L Q_1^{(l)} Q_1^{(n)*} + \varepsilon_R \mu_R Q_N^{(l)} Q_N^{(n)*} \right\} Q_k^{(n)*} \right], \quad (48)$$

$$j_{k,k+1} = 2J \sum_{l,n=1}^N \text{Im} \left[\frac{1}{2i(\lambda^{(l)} - \lambda^{(n)*})} Q_k^{(l)} \left\{ \varepsilon_L \mu_L Q_1^{(l)} Q_1^{(n)*} + \varepsilon_R \mu_R Q_N^{(l)} Q_N^{(n)*} \right\} Q_{k+1}^{(n)*} \right], \quad (49)$$

where $\lambda^{(l)}$ and $Q_k^{(l)}$ are given by (46,47). After some calculations, we arrive at the following simple formulas for the magnetization and the spin current for steady state (The detailed calculations are written in Appendix A.).

$$m_k^z = \mu_L - bD_k^{(L)} = \mu_R + bD_k^{(R)}, \quad j = \frac{2Jlr(\mu_L - \mu_R)}{(1+lr)(l+r)}, \quad (50)$$

where $l = \varepsilon_L/4J$, $r = \varepsilon_R/4J$, $b = j/2J$ and $D_k^{(L)}$ and $D_k^{(R)}$ are defined as

$$D_1^{(L)} = l^{-1}, \quad D_k^{(L)} = l + l^{-1}, \quad (2 \leq k \leq N-1), \quad D_N^{(L)} = l + l^{-1} + r, \quad (51)$$

$$D_1^{(R)} = r + r^{-1} + l, \quad D_k^{(R)} = r + r^{-1}, \quad (2 \leq k \leq N-1), \quad D_N^{(R)} = r^{-1}, \quad (52)$$

Our formulas for the magnetization and the spin current are valid for all parametric values of $\mu_{L/R}$, $\varepsilon_{L/R}$, and agree with the results in [32–34] obtained by MPA for the case of the antisymmetric magnetization on reservoirs ($\mu_L = -\mu_R$). For Fig.2, we confirm that our formula (50-52) for magnetization and spin current for steady state coincide with the ones obtained by MPA [32–34] (when $\mu_L = -\mu_R$).

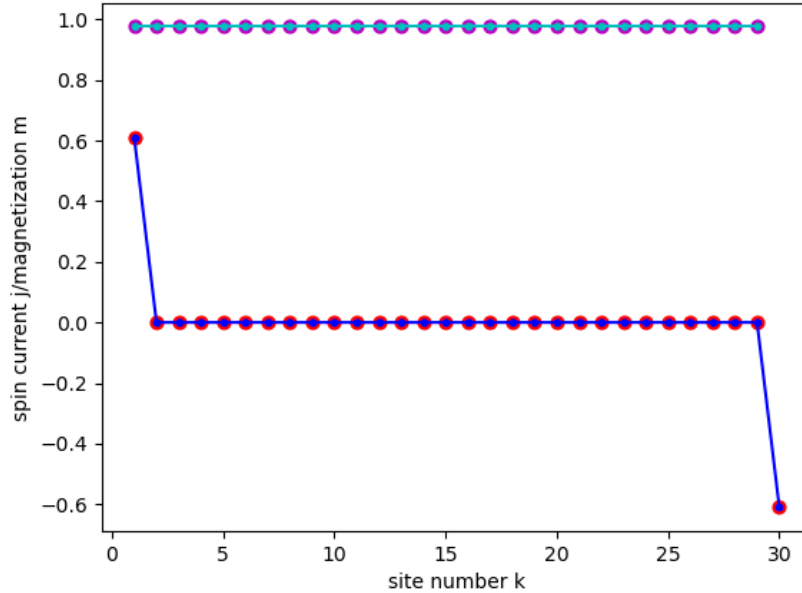


FIG. 2. Magnetization (red dots and blue line) and spin current for steady state (The parameters set $N = 30$, $J = 1.0$, $B = 0.0$, $\varepsilon_{L/R} = 5$ and $\mu_L = -\mu_R = 1$. The red dots and blue line are the magnetization for steady state obtained by our formula (50-52) and MPA solution obtained in [32–34], respectively, and the magenta dots and cyan line are the spin current for steady state obtained by our formula (50-52) and MPA solution obtained in [32–34], respectively.)

Our formulas (50-52) are the most general solution for the magnetization and the spin current in steady state for the open XX spin chain with boundary dissipation in the sense that they are valid for all parametric values of $\mu_{L/R}$, $\varepsilon_{L/R}$. It is also interesting to consider whether our results for the general parameters case can also be realized in terms of MPA.

IV. THE DYNAMICS OF PHYSICAL OBSERVABLES

Analytical studies for open quantum systems with Lindblad dynamics for large systems have been challenging in terms of the diagonalization of the Lindbladian. The exact solution for open quantum systems has been studied by using other procedures. For the open XX spin chain with boundary dissipation, the solutions in steady state are obtained by using MPA [32–34], but the dynamics have been much less understood analytically. Since we obtain the analytical formula for the time-dependence of magnetization (44) and spin current (45), the study for those behaviors becomes easier.

A. Behaviors of time-dependent physical observables

We first evaluate our formulas (44,45) numerically and observe several behaviors for the time-dependence of the magnetization and the spin current for the open XX chain. We will examine them analytically in subsequent discussions. In Fig.3, spatio-temporal regions where the magnetization is large are displayed. We observe a clear and interesting light-cone structure. In Fig.4, the time-dependence of the magnetization and the spin current are plotted for several fixed-site k . We observe several specific behaviors depending on the position of a site in the system. Some of them can be understood from the light-cone structure in Fig.3 but others need further considerations. At sites near a boundary, the magnetization and the spin current show a plateau regime as in Fig.4(b) and 4(e). The plateau regime means the quasi-stabilized regime in which the magnetization almost does not change over a duration of time before the magnetization reaches its steady state value and appears as soon as the time evolution starts. This is consistent with the light-cone structure in Fig.3. On the other hand, at a site near the center of the chain, the magnetization shows a much slower convergence to the steady state value than that near a boundary, compare Fig.4(a) with Fig.4(b).

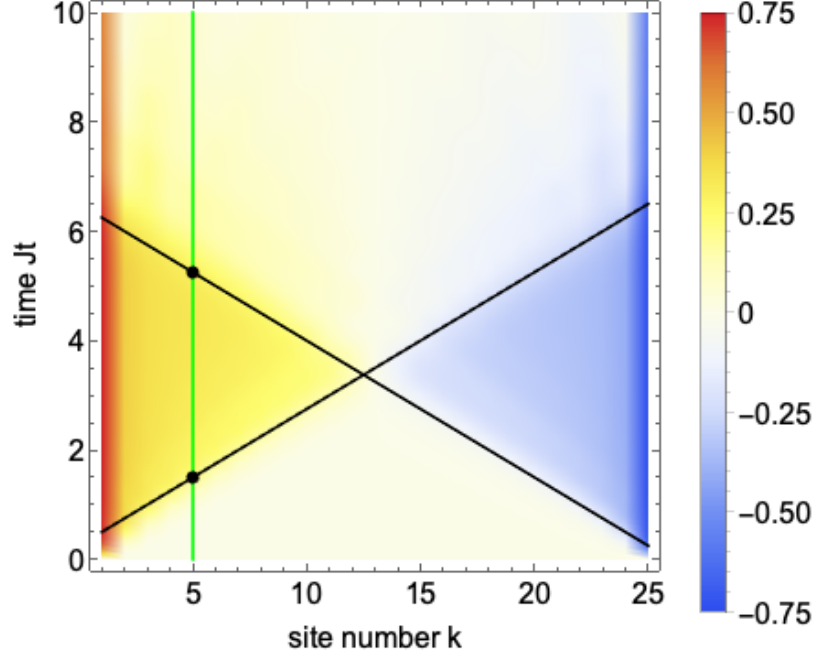


FIG. 3. Spatio-temporal dependence of the local magnetization by (44). The parameters are set to $N = 25$, $\varepsilon_{L/R} = 5.0$, $J = 1.0$, $B = 0.0$, $\mu_L = -\mu_R = 1.0$, $\varepsilon_{L/R} = 5.0$. The black lines are $Jt = (k+1)/4$ and $Jt = (N-k+1)/4$ which represent the initial and final time of the plateau regime. The points at the intersection of the green and black lines are the initial and final time of the plateau regime at the site 5. We show the detail of the analysis of the plateau regime later in this section.

Also, at a bulk site which is not close to the center of the chain, we observe a plateau regime which is shorter than that near a boundary. This is not only due to the shape of the light cone but also because there appear oscillatory behaviors at the beginning of the plateau. Convergence to the steady state value becomes slow, as the site gets closer to the center of the chain. In the following, we first analytically discuss the light-cones structure in Fig.3 using the analogy to that in closed systems. Second, we consider the relation between the slow convergence for the magnetization on a bulk site and the Liouvillian gap. Lastly, we consider the issue of the plateau regime.

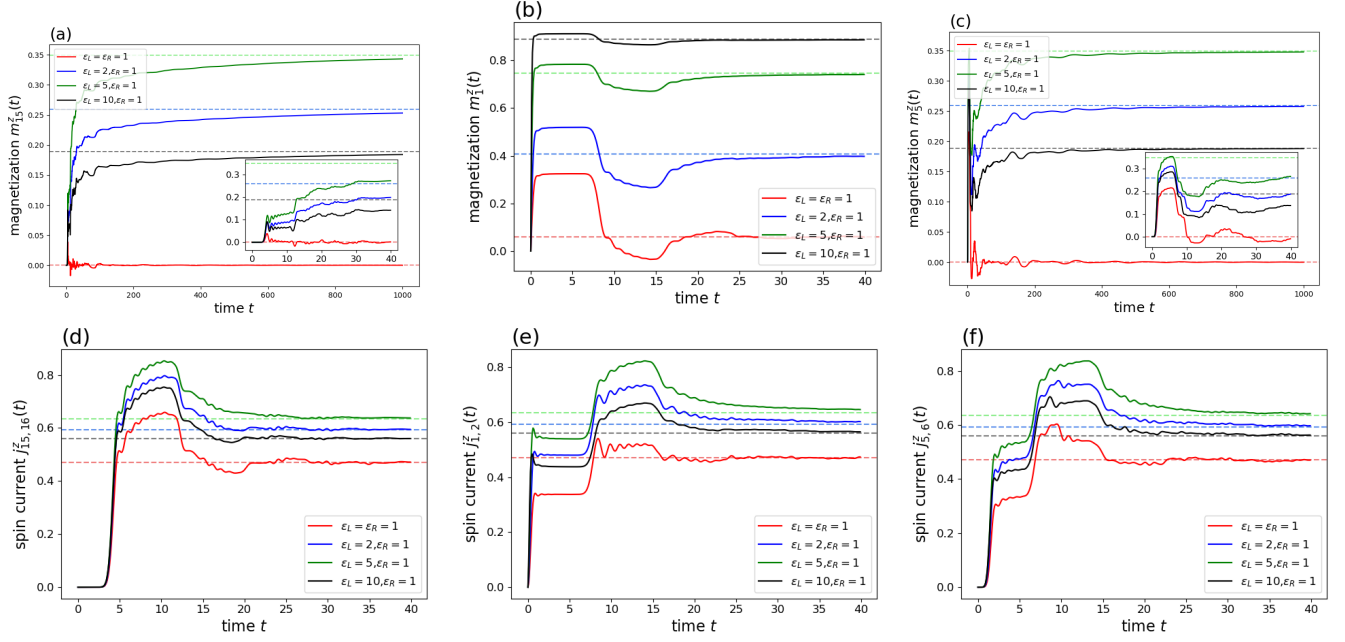


FIG. 4. Time-dependence of physical observables by (44,45). We observe behaviors of the time-dependence of the magnetization and spin current when the dissipative strength ε_L are changed in (a), (b), (d) and (e), where the red, blue, green and black curves correspond to $\varepsilon_L = 1.0, 2.0, 5.0, 10.0, \varepsilon_R = 1.0$ cases, respectively. (a) and (d): The time-dependence of the magnetization and the spin current at the center site ($k = 15$). (b) and (e): The time-dependence of the magnetization and the spin current near the left boundary ($k = 1$). (c) and (f): The time-dependence of the magnetization and the spin current at the bulk site ($k = 5$). Other parameters in these pictures are set to $N = 30, J = 1.0, B = 0.0, \mu_L = -\mu_R = 1.0$. The light color dotted lines are the magnetization and spin current in the steady state.

B. Light-cone structure

For quench dynamics in closed systems which exchange energy with external reservoirs, it has been observed that frontiers of the magnetization show a light-cone structure due to the Lieb-Robinson bounds, and the slope of the light-cone is determined from the maximum velocity[11, 56, 69, 70]. In particular, for the quench dynamics in the closed XX spin chain, the slope of the light-cone corresponds to the velocity of the free magnon propagation, and the propagating velocity can be calculated as the group velocity $|v| = |d\varepsilon(k)/dk|$ from the dispersion relation $\varepsilon = \varepsilon(k)$ of the one particle excitation[57, 70], where k is a momentum, and $\varepsilon(k)$ is an eigenenergy.

The slope of the light-cones in Fig.3 for our open XX spin chain may be determined by using an analogy to the quench dynamics in the closed XX spin chain discussed above. More precisely we may conjecture that the slope of the light-cones in Fig.3 is given by a formula,

$$|v| = \left| \frac{d(2\lambda^{(l)})}{d\theta_l} \right| = |4J \sin \theta_l|, \quad (53)$$

where λ_l is the eigenvalue of the matrix Ξ (20,22) and θ_l is determined as (24). The factor 2 in front of λ_l in (53) may be attributed to the same factor in (34), which could be absorbed in the definition of Majonara fermion operator by changing the inner product which the operator space \mathcal{K} is orthonormal with respect to[46, 49]. At $\theta_l \approx \pi/2$, the velocity approaches the maximum $|v|_{\max} = 4J$, and the eigenmode reaches the furthest site from a boundary. Thus the slope of the sharp front in Fig.3 is supposed to be a quarter with the dimensionless time unit Jt in Fig.3, and this is numerically indeed confirmed.

Moreover, by carefully examining our formula (44), one sees that time-dependence of the magnetization can be interpreted as a result of propagation of effects of boundary dissipations. At an arbitrary site k , the propagation of the effect of either boundary dissipation repeats reflecting at the other boundary after passing the site k . While repeating such a propagation of the effect of the boundary dissipations, the magnetization converges to the one in steady state. This picture can be understood by our formulas (44,45). We consider the fluctuation from the steady

state for the magnetization at the site k as the following,

$$\left| m_k^z(t) - m_k^{z,\text{NESS}} \right| = \left| \sum_{l,n=1}^N \text{Re} \left[\frac{e^{-2it(\lambda^{(l)} - \lambda^{(n)*})}}{2i(\lambda^{(l)} - \lambda^{(n)*})} Q_k^{(l)} \left\{ \varepsilon_L \mu_L Q_1^{(l)} Q_1^{(n)*} + \varepsilon_R \mu_R Q_N^{(l)} Q_N^{(n)*} \right\} Q_k^{(n)*} \right] \right|. \quad (54)$$

For large system size N , the term $e^{-2it(\lambda^{(l)} - \lambda^{(n)*})} Q_k^{(l)} Q_{1(N)}^{(l)} Q_{1(N)}^{(n)*} Q_k^{(n)*}$ can be rewritten by using (23) and the de Moivre's theorem into

$$e^{-2it(\lambda^{(l)} - \lambda^{(n)*})} Q_k^{(l)} Q_1^{(l)} Q_1^{(n)*} Q_k^{(n)*} \propto (e^{i(k\theta_l - 2\lambda^{(l)}t)} + e^{-i(k\theta_l + 2\lambda^{(l)}t)})(e^{i(k\theta_n + 2\lambda^{(n)*}t)} + e^{-i(k\theta_n^* - 2\lambda^{(n)*}t)}), \quad (55)$$

$$e^{-2it(\lambda^{(l)} - \lambda^{(n)*})} Q_k^{(l)} Q_N^{(l)} Q_N^{(n)*} Q_k^{(n)*} \propto (e^{i((N-k)\theta_l - 2\lambda^{(l)}t)} + e^{-i((N-k)\theta_l + 2\lambda^{(l)}t)})(e^{i((N-k)\theta_n + 2\lambda^{(n)*}t)} + e^{-i((N-k)\theta_n^* - 2\lambda^{(n)*}t)}). \quad (56)$$

Therefore, the term $e^{-2it(\lambda^{(l)} - \lambda^{(n)*})} Q_k^{(l)} Q_{1(N)}^{(l)} Q_{1(N)}^{(n)*} Q_k^{(n)*}$ is rewritten as the product of the parts which are derived from the time-evolution for a state and its dual state, and contributions of the left and right boundaries are interpreted as a superposition of incident waves and reflected waves which spread with group velocities, respectively. The value of the group velocity v_g is calculated from (55,56) to be

$$v_g = \frac{\Delta k}{\Delta t} = \frac{\Delta(2\lambda^{(l)})}{\Delta\theta_l} \approx \frac{d(2\lambda^{(l)})}{d\theta_l}, \quad (57)$$

which is nothing but (53). Thus, we have demonstrated that the light-cone structure of the magnetization observed in Fig.3 can be analytically understood as a result of propagations of effects of the boundary dissipations from our formulas (44,45).

C. The relation between a slow convergence and the Liouvillian gap

Next, we consider a relation between the slow convergence of the magnetization at a bulk site near the center of the system and the Liouvillian gap Δ . Asymptotic behaviors for long time of time-dependence of physical observables after long time are expected to be characterized by the eigenmode corresponding to the Liouvillian gap, and the relaxation time τ is determined as the inverse of the double of the Liouvillian gap Δ which is defined in this system as

$$\Delta = -2 \max \text{Im}[\lambda^{(k)}], \quad (58)$$

where $\lambda^{(k)}$ is the eigenvalue of the matrix Ξ which defined as (22,24). In Fig.5(a), we show semi logarithmic plots of the difference of the magnetization at time t to its asymptotic value, where we observe that its asymptotic behaviors at an arbitrary site k becomes an exponential decay. In our numerical results, the inverse of the relaxation times $1/\tau$ which are obtained by fitting to the data for the time-dependence of the magnetization from $t = 500$ to $t = 1000$ using our formula (44) are $1.71_7 \times 10^{-3}$ ($\varepsilon_L = 2.0, \varepsilon_R = 1.0$), $2.03_5 \times 10^{-3}$ ($\varepsilon_L = 5.0, \varepsilon_R = 1.0$), and $1.67_5 \times 10^{-3}$ ($\varepsilon_L = 2.0, \varepsilon_R = 1.0$), which should be compared to twice the Liouvillian gaps $2\Delta = 1.72_1 \times 10^{-3}$ ($\varepsilon_L = 2.0, \varepsilon_R = 1.0$), $2.04_1 \times 10^{-3}$ ($\varepsilon_L = 10.0, \varepsilon_R = 1.0$), and $1.67_8 \times 10^{-3}$ ($\varepsilon_L = 10.0, \varepsilon_R = 1.0$) computed using (58). We see that the relaxation time τ for these exponential decay are almost the same as the inverse of the double of the Liouvillian gap $\tau \approx 1/2\Delta$. The slow convergence which is observed in Fig.4(a) is related to the eigenmode corresponding to the Liouvillian gap.

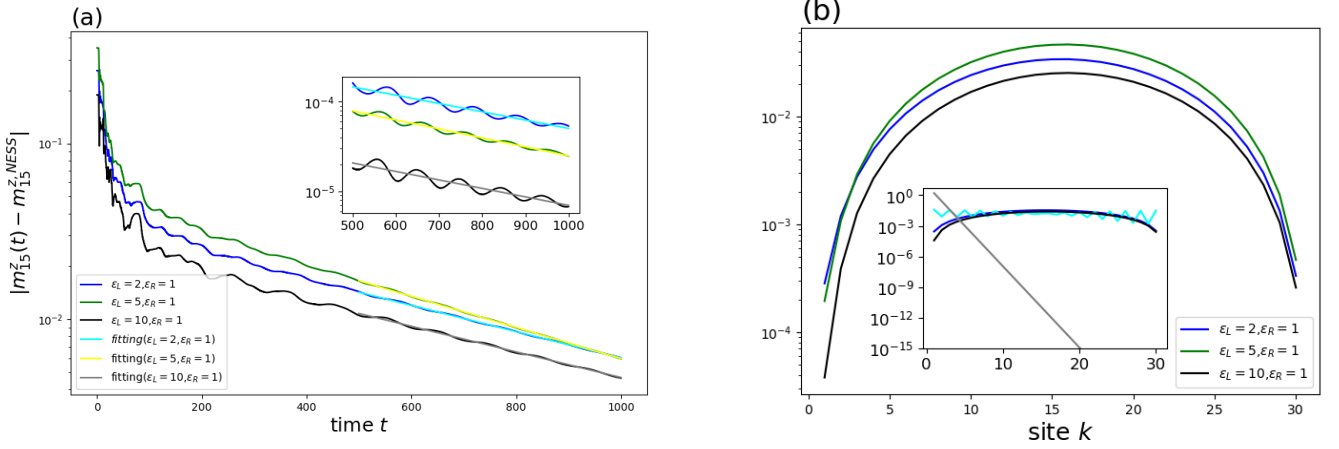


FIG. 5. Asymptotic behavior of the magnetization after long time: (a) The time-dependence of the magnetization at the site $k = 15$. The inserted figure is the time-dependence of the magnetization at the site 1 and the function fitting to exponential. The cyan, yellow and gray lines represent the fittings to exponential decays. The values of their slopes are given in the text. (b) The coefficient for the eigenmode corresponding to the Liouvillian gap and the special eigenvalues (27). In the inserted figure, the blue and cyan curves ($\varepsilon_L = 2, \varepsilon_R = 1$) are the coefficients for the eigenmode corresponding the Liouvillian gap and the eigenvalue with the largest value of the imaginary part which becomes the special eigenvalue when $\varepsilon_{L/R} > 4J$. The black and gray curves ($\varepsilon_L = 10, \varepsilon_R = 1$) are the coefficients for the eigenmode corresponding the Liouvillian gap and the special eigenvalue. Other parameters in these figures are set to $N = 30, J = 1.0, B = 0.0, \mu_L = -\mu_R = 1.0$.

The Liouvillian gaps for open quantum systems have not been much discussed analytically, though they have been calculated numerically or by using an analogy from infinitely closed systems in a few previous works. For example the Liouvillian gap for open transverse Ising spin chain and XY spin chain has been estimated by the asymptotic result using analogy from infinitely closed systems[46, 47, 71]. For our case of open XX spin chain, we can estimate the magnitude of the Liouvillian gap Δ by using the exact spectrum of the Lindbladian for a finite-size system obtained in section 2. The angle θ_k in the eigenvalue $\lambda^{(k)}$ which defined as (22,24) is separated as $\theta_k = \frac{k}{N+1}\pi + \eta_k$ where $\eta_k \sim \mathcal{O}(N^{-2})$, and we define the values $\delta_k \equiv \text{Re}[\eta_k]$, and $\xi_k \equiv \text{Im}[\eta_k]$ ($\delta_k, \xi_k \sim \mathcal{O}(N^{-2})$). Then, we can calculate the Liouvillian gap exactly and estimate its asymptotic behavior to be

$$\begin{aligned} \Delta &= -2 \max \left[\sin \left(\frac{\pi}{N+1} + \delta_k \right) \sinh \xi_k \right] \\ &= -2 (N^{-1} + N^{-2} + \dots) (N^{-2} + N^{-3} + \dots) \sim N^{-3}. \end{aligned} \quad (59)$$

Since the slope of the lines in Fig.5(a) is estimated as the double of the Liouvillian gap 2Δ by exponential fitting and the Liouvillian gap is estimated as $\Delta \sim N^{-3}$, the relaxation time τ for the magnetization at a site near the center of the chain can be estimated to behave as $\tau \sim N^3$, and the slow convergence in Fig.4(a) is characterized by the eigenmode corresponding to the Liouvillian gap Δ .

On the other hand, the magnetization on a site near a boundary seems to converge faster than the one at a site near the center of the chain in Fig.4(b). Whether the slow convergence occurs or not is determined by the trade-off between the coefficients $Q_k^{(l)} \left\{ \varepsilon_L \mu_L Q_1^{(l)} Q_1^{(n)*} + \varepsilon_R \mu_R Q_N^{(l)} Q_N^{(n)*} \right\} Q_k^{(n)*}$ in (44) for the eigenmode corresponding to the Liouvillian gap Δ and the one corresponding to the largest value of the imaginary part which becomes the special eigenvalue when $\varepsilon_{L/R} > 4J$. In Fig.5(b), we compare the coefficient for the eigenmode corresponding to the Liouvillian gap with the one corresponding to the largest value of the imaginary part which becomes the special eigenvalue when $\varepsilon_{L/R} > 4J$. We observe that the former is smaller than the latter near a boundary and the former is larger than the latter near the center. In particular, when $\varepsilon_L \gg 4J$, the former on a site near a boundary is as small as we can neglect compared with the latter. Similarly the latter on a bulk site is as small as we can neglect compared with the former. This explains why we observe the rapid convergence on a site near a boundary and the slow convergence on a site near the center of the chain.

D. The emergence of the plateau regime near a boundary

Lastly, for understanding behaviors of the plateau regime, it is useful to consider the time derivative of the magnetization. Since the magnetization in the plateau regime does not change over a duration of time t , the time derivative of the magnetization becomes zero during the plateau regime. Thus, we can expect to estimate the plateau time τ_p defined as a duration of time that magnetization does not change using the analysis of the time derivative of the magnetization. A time derivative of magnetization for the site k can be calculated from (44) as

$$\mu_k(t) := \frac{\partial m_k}{\partial t} = \varepsilon_L \mu_L \left| \sum_{l=1}^N e^{-2it\lambda^{(l)}} Q_1^{(l)} Q_k^{(l)} \right|^2 + \varepsilon_R \mu_R \left| \sum_{l=1}^N e^{-2it\lambda^{(l)}} Q_N^{(l)} Q_k^{(l)} \right|^2. \quad (60)$$

The first and the second terms in the time derivative of the magnetization (60) will be called the left and right dissipation contributions, respectively. After some calculations (see Appendix.B for details), we obtain the time derivative of magnetization $\mu_k(t)$ for large system $N \gg 1$ as

$$\mu_k(t) \approx \varepsilon_L \mu_L (f_{\text{no}}(1, k; t) - f_{\text{sp}}(1, k; t))^2 + \varepsilon_R \mu_R (f_{\text{no}}(N, k; t) - f_{\text{sp}}(N, k; t))^2, \quad (61)$$

where the functions $f_{\text{no}}(n, m; t)$ and $f_{\text{sp}}(n, m; t)$ are the parts of the normal eigenstates and the special eigenstates corresponding to the normal and special eigenvalues for the matrix Ξ (20), respectively. These functions are calculated as

$$f_{\text{no}}(n, m; t) \equiv \frac{8J^2}{\varepsilon_L} \left(\int_t^\infty ds e^{-2J\left(\frac{\varepsilon_L}{4J} - \frac{4J}{\varepsilon_L}\right)(t-s)} Y_{n,m}(4Js) - \int_{-\infty}^t ds e^{-2J\left(\frac{\varepsilon_L}{4J} - \frac{4J}{\varepsilon_L}\right)(t-s)} Y_{n,m}(4Js) I\left(\frac{\varepsilon_L}{4J}\right) \right) + ((-1)^{n+m} - (-1)^n \delta_{n,m}) \delta_{\frac{\varepsilon_L}{4J}, 1}, \quad (62)$$

$$f_{\text{sp}}(n, m; t) \equiv e^{-2J\left(\frac{\varepsilon_L}{4J} - \frac{4J}{\varepsilon_L}\right)t} \left(1 + \left(\frac{\varepsilon_L}{4J}\right)^2 \right) \left(-\frac{\varepsilon_L}{4J}\right)^{-n-m} I\left(\frac{\varepsilon_L}{4J}\right) + (-1)^{N+1} e^{-2J\left(\frac{\varepsilon_R}{4J} - \frac{4J}{\varepsilon_R}\right)t} \left(1 + \left(\frac{\varepsilon_R}{4J}\right)^2 \right) \left(\frac{\varepsilon_R}{4J}\right)^{-2N-2+n+m} I\left(\frac{\varepsilon_R}{4J}\right), \quad (63)$$

where the function $I(x)$ takes the value 1 if $x > 1$ and 0 if $x \leq 1$, and we define the function $Y_{n,m}(t)$ as

$$Y_{n,m}(t) = (-1)^m J_{n-m}(t) - J_{n+m}(t) + \frac{\varepsilon_L}{4J} (2J_{n+m-1}(t) + (-1)^m J_{n-m+1}(t) - (-1)^m J_{n-m-1}(t)) - \frac{\varepsilon_L^2}{16J^2} (J_{n+m-2}(t) + (-1)^m J_{n-m}(t)). \quad (64)$$

Now, we carefully examine the functions (62-64). The function $Y_{n,m}(t)$ (64) is the sum of the Bessel functions of the first kind, and its behavior is important for discussing behaviors of the part of the normal eigenstates. The Bessel function $J_\alpha(x)$ has the following series expansion,

$$J_\alpha(x) = \sum_{n=0}^{\infty} \frac{(-1)^n}{n! \Gamma(n + \alpha + 1)} \left(\frac{x}{2}\right)^{2m+\alpha}. \quad (65)$$

Thus, the part of the normal eigenstates f_{no} is the sum of the products of monomials and the exponential function of the form $(2Jt)^{2m+\alpha} e^{-2Jt\left(\frac{\varepsilon_L}{4J} - \frac{4J}{\varepsilon_L}\right)}$. On the other hand, since the part of the special eigenstates f_{sp} and the cross terms between the part of the special and normal eigenstates $f_{\text{sp}} f_{\text{no}}$ behaves exponentially, these decay more rapidly than the part of the normal eigenstates. This implies that the contribution of the part of the special eigenstates is much smaller than the one of the part of the normal eigenstates except near the initial time, and the part of the special eigenstates f_{sp} (63) and the cross terms between the part of the special and normal eigenstates $f_{\text{sp}} f_{\text{no}}$ do not contribute to the formalization of the plateau regime.

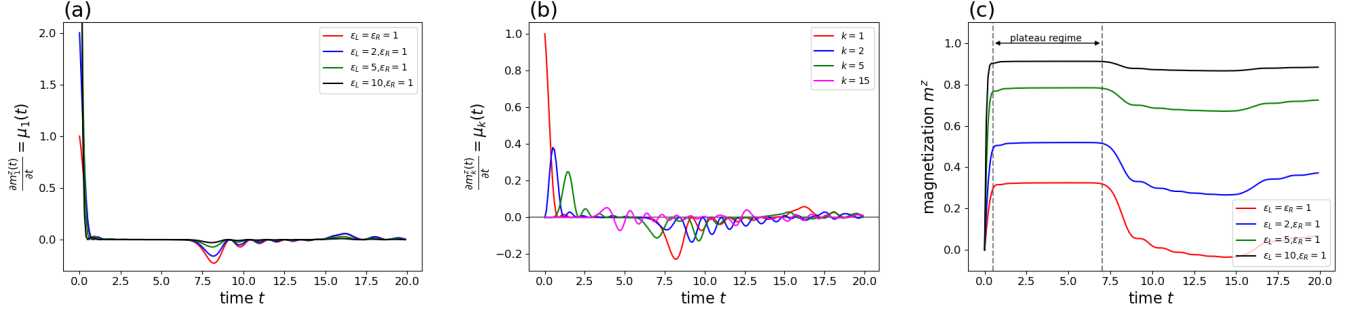


FIG. 6. Time-dependence of the time derivative of magnetization at a boundary and bulk: (a) dependence for the dissipative strength at the left boundary for the case of $\varepsilon_L = 1.0, 2.0, 5.0, 10.0, \varepsilon_R = 1.0$. (Other parameters set $N = 30, J = 1.0, B = 0.0, \mu_L = -\mu_R = 1.0$.), (b) dependence for the position of site k for the case of $k = 1, 2, 5, 10$. (Other parameters set $N = 30, J = 1.0, B = 0.0, \varepsilon_{L/R} = 1.0, \mu_L = -\mu_R = 1.0$.), (c) the plateau regime on the left boundary ($k = 1$) (Other parameters set $N = 30, J = 1.0, B = 0.0, \mu_L = -\mu_R = 1.0$.). The two vertical dot lines are the initial and final time for the plateau regime which are obtained as $t_i = (k + 1)/4J$, $t_f = (N - k - 1)/4J$ from the calculation for the time-derivative of the magnetization (61-64).

Since the left and right dissipation contributions in the time derivative of magnetization $\mu_k(t)$ are separated as (61), we can consider these contributions individually. Moreover, each term includes the part of the normal eigenstates f_{no} and the part of the special eigenstates f_{sp} . We will consider each part individually. Considering above, since the part of the special eigenstates f_{sp} in (63) and the cross terms between the part of the special and normal eigenstates $f_{\text{sp}}f_{\text{no}}$ do not contribute to the formalization of the plateau regime, we only focus on the part of the normal eigenstates f_{no} .

The functions $f_{\text{no}}(1, k; t)$ and $f_{\text{no}}(N, k; t)$ in (62) in the time derivative of magnetization $\mu_k(t)$ in (61) is constructed by the integral of the product of the exponential function $e^{-2J\left(\frac{\varepsilon_L}{4J} - \frac{4J}{\varepsilon_L}\right)(t-s)}$ and the function $Y_{1(N),k}(4Js)$. Moreover, Since the function $Y_{1(N),k}(4Js)$ is the sum of the Bessel function of the first kind defined as (65), we can understand the contribution to the behavior of the time derivative of magnetization $\mu_k(t)$ (61) by using property of the Bessel function of the first kind such as the asymptotic behavior of the Bessel function of the first kind of the α -th order $J_\alpha(x)$ is $J_\alpha(x) \approx \frac{1}{\Gamma(\alpha+1)}x^k$ around $x \sim 0$ [72], and the fact that the Bessel function $J_\alpha(x)$ is close to zero when $x \lesssim k$. By this later property, the behavior of the function $Y_{1,k}(4Js)$ (64) changes when $4Js = \max(0, k - 2), k + 1$. When $0 \leq 4Jt < \max(0, k - 2)$, the function $Y_{1,k}(4Js)$ is close to zero. When $\max(0, k - 2) \leq 4Jt < k + 1$, the only terms including J_{k-1}, J_{k-2}, J_k in the function $Y_{1,k}(4Js)$ are non-zero. When $k + 1 \leq 4Jt$, the all terms in the function $Y_{1,k}(4Js)$ become non-zero, but the part of the normal eigenstates $f_{\text{no}}(1, k; t)$ (62) becomes almost zero. Since the magnitude of integrated function in the part of the normal eigenstates $f_{\text{no}}(n, m; t)$ decays exponentially with the relaxation time $\left(2J\left(\frac{\varepsilon_L}{4J} - \frac{4J}{\varepsilon_L}\right)\right)^{-1}$, this is close to zero, and the part of the normal eigenstates $f_{\text{no}}(n, m; t)$ is also close to zero. Similarly, the behavior of the function $Y_{N,k}(4Js)$ included in the left dissipation contribution for the time derivative of magnetization $\mu_k(t)$ changes when $4Js = N - k - 1, N + k$.

From the above analysis and Fig.6, we can examine that the plateau time τ_p is independent of boundary dissipative parameters $\varepsilon_{L/R}, \mu_{L/R}$, and depends on system-size N and the position of site k observing in Fig.4 and 7, and obtain the fact that the time derivative of the magnetization $\mu_k(t)$ is mostly always equal to zero between $t = \frac{k+1}{4J}$ and $t = \frac{N-k-1}{4J}$. When a time derivative of magnetization is equal to zero, the magnetization does not change over a duration of time at time t . Thus, we can regard the plateau regime as the duration of time between $t = \frac{k+1}{4J}$ and $t = \frac{N-k-1}{4J}$, and obtain the plateau time $\tau_p = \left\lfloor \frac{N-k-1}{4J} \right\rfloor$. Since the plateau time decreases to zero as the site becomes closer to the center of the system, the plateau regime is clearly observed for sites near a boundary.

This change in the plateau regime can be understood by the analysis of the light-cone structure. The light-cones show the frontier of the propagation of the effect of the boundary dissipations. After the effect of a boundary dissipation passes the site k , the state at the site k will be stabilized for a while. However, when the effect of dissipation at the other boundary reaches the site k , stability at the site k is lost. For bulk sites near the center, the times at which the effects of the two boundaries are close, so that the plateau time becomes short. The initial time and final time of the plateau regime at a fixed site k are represented as the boundaries of the light-cones in Fig.3 at the site k , and the red or blue part in Fig. 3 shows the plateau regime. A light-cone can spread indefinitely in quench dynamics[70], but not in the open XX spin chain due to the presence of boundaries. Thus, the plateau regime is a phenomenon which appears due to a combination of light-cone structures, similar to the ones in a closed system, and the reflections of them at the boundaries. As such the plateau regime can be kept only in a finite duration of time. Since there is not

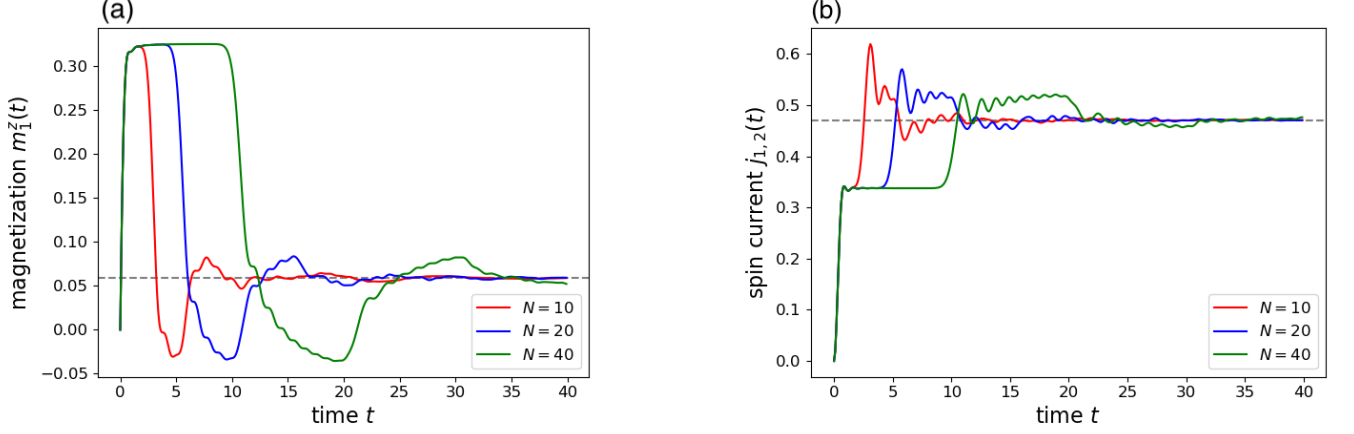


FIG. 7. The system-size dependence for the time-dependence of the magnetization (a) and spin current (b) on the left boundary ($k=1$). Other parameters in these pictures are set to $J=1.0$, $B=0.0$, $\varepsilon_L = \varepsilon_R = 1.0$, $\mu_L = -\mu_R = 1.0$. The gray dotted line is the magnetization and spin current in the steady state.

such a quasi-stabilized regime in a dynamics in quench dynamics for the closed XX spin chain, we may say that the plateau regime is one of the specific phenomena for the open quantum XX spin chain.

Also, the height of the plateau regime can be calculated by using the time-derivative of the magnetization $\mu_k(t)$ (61). Since the height of the plateau regime depends on either the left or right contribution to the time derivative of the magnetization $\mu_k(t)$ (61), we only consider the left half of the system. In this case, the height of the plateau regime at the site k $H_p(J, \varepsilon_L, \mu_L; k)$ is estimated as

$$H_p(J, \varepsilon_L, \mu_L; k) \approx \varepsilon_L \mu_L \int_0^{\frac{k+1}{4J}} dt (f_{\text{no}}(1, k; t) - f_{\text{sp}}(1, k; t))^2, \quad (66)$$

where we define the functions $f_{\text{no}}(1, k; t)$, $f_{\text{sp}}(1, k; t)$ in (62,63). This estimation is almost exact, but causes a little error by the finite-size effect. The plateau regime may be interpreted as the quasi-steady state where the magnetization seems not to change over a duration of time t formed by the left or right dissipation, but a physical meaning of its height is not very clear for the moment.

Thus, our formulas for the time-dependence of the magnetization and the spin current (44,45) can examine an arbitrary behavior for all time. When one applies our approach to other physical observables, for example energy, correlation function and susceptibility, one can understand behaviors of the physical observables analytically.

V. CONCLUSION

We have applied the general procedure of the third quantization to the open XX spin chain. We find that the structure matrix of the open XX spin chain is diagonalizable analytically. Moreover, we find that although the structure matrix is ordinarily decomposed into $2N \times 2N$ matrix, the structure matrix for the open XX spin chain is decomposed into $N \times N$ non-Hermitian matrix, and the eigenvalues and eigenvectors of this non-Hermitian matrix are calculated analytically. The eigenvalue distribution of this non-Hermitian matrix changes dramatically with the increment of boundary dissipative strength. If a dissipative strength is larger than four times the coupling constant between sites on the system, we could find the emergence of a special eigenvalue which is a larger imaginary part than the others. Since the open XX spin chain is diagonalizable, we can exactly calculate time-evolution from a general initial condition including the thermal equilibrium state. We obtain the linear differential equation for the correlation matrix which is constructed from the expectation value of the product of two Majorana operators. The several components of the correlation matrix correspond to magnetization on the site k and spin current between the site k and $k+1$.

The exact solutions of time-dependent magnetization on arbitrary site k and spin current between arbitrary sites k and $k+1$ are the main results in this study. These formulas also include the solutions for NESS which is defined as $t \rightarrow \infty$. Our analytical formulas for magnetization and spin current in steady state generalize the ones obtained by the MPA solutions for the special case of antisymmetric magnetization on reservoirs [32–34]. Evaluating the

exact solutions of time-dependent magnetization on arbitrary site k and spin current between arbitrary sites k and $k + 1$ numerically, we observe some specific behaviors. Using our formulas, we can examine these analytically. The spatio-temporal regions where the magnetization is large are displayed. We observe a clear and interesting light-cone structure. We conjecture that the slope of the light-cones for our open XX spin chain may be determined by using an analogy to the quench dynamics in the closed XX spin chain. At a site near the center of the chain, the magnetization shows a much slower convergence to the steady state value than that near a boundary. The decay rate of this slow convergence is estimated by the Liouvillian gap. Whether the slow convergence occurs or not is determined by the trade-off between the magnitude of the contribution of the eigenmode corresponding to the Liouvillian gap and the one corresponding to the largest value of the imaginary part which becomes the special eigenvalue when $\varepsilon_{L/R} > 4J$. The time-dependent magnetization at the site near a boundary and spin current between the sites near a boundary exhibit specific behaviors before the system reaches steady state. They do not approach the steady state values exponentially or by power-law but approach the steady state with oscillation after finishing the plateau regime. The plateau regime means that magnetization does not change over a duration of time before the magnetization reaches its steady state value. The plateau time is defined as the duration of time that magnetization does not change. When we consider the time-derivative of magnetization, this derivative takes the form of the product of Bessel function and exponential function. For this analysis, we find there is the duration of time over which this derivative is equal to zero. We verify the existence of the plateau regime and the plateau time depends on the system size N and site number k . This behavior always occurred despite the existence of special eigenvalues, and is independent of the boundary dissipation strength.

It is important that one can obtain the exact formula for the time-dependence of physical observables analytically. Applying this fact, higher-order physical observables will be calculated analytically. Moreover, since the Lindbladian map takes Jordan canonical form in an arbitrary quadratic fermion chain, XY spin chain, XX spin chain with homogeneous bulk dissipation and long-range interaction systems can be analyzed. Though we can discuss the exact behaviors of the physical observables for an arbitrary time for the open XX spin chain by our analysis, we did not find a phase transition. However, the phase transition has been studied in the context of the analysis of the non-Hermitian systems which is applied to the open quantum systems. In future studies, we hope to find new non-Hermitian phenomena for our system and others beyond the post-selection which usually approximates in the context of non-Hermitian physics.

ACKNOWLEDGMENTS

The authors are grateful to T. Fukadai and Y. Nakanishi for useful discussions. The work of TS is supported by JSPS KAKENHI Grants No. JP16H06338, No. JP18H01141, No. JP18H03672, No. JP19L03665.

Appendix A: Physical observables for steady state

In the main part of the paper, we find formulas for magnetization and spin current for steady state as follows,

$$m_k^z = \sum_{l,n=1}^N \text{Re} \left[\frac{1}{2i(\lambda^{(l)} - \lambda^{(n)*})} Q_k^{(l)} \left\{ \varepsilon_L \mu_L Q_1^{(l)} Q_1^{(n)*} + \varepsilon_R \mu_R Q_N^{(l)} Q_N^{(n)*} \right\} Q_k^{(n)*} \right], \quad (\text{A1})$$

$$j_{k,k+1} = 2J \sum_{l,n=1}^N \text{Im} \left[\frac{1}{2i(\lambda^{(l)} - \lambda^{(n)*})} Q_k^{(l)} \left\{ \varepsilon_L \mu_L Q_1^{(l)} Q_1^{(n)*} + \varepsilon_R \mu_R Q_N^{(l)} Q_N^{(n)*} \right\} Q_{k+1}^{(n)*} \right], \quad (\text{A2})$$

where eigenvector $\beta_j = i\lambda^{(j)}$ and the component of eigenvector $Q_k^{(j)}$ is obtained (22,23), and the parameter θ_j satisfies the conditional equation (24). Then, separating left and right boundary contributions,

$$m_{k,L}^z = \varepsilon_L \mu_L \sum_{l,n=1}^N \operatorname{Re} \left[\frac{1}{2i(\lambda^{(l)} - \lambda^{(n)*})} Q_k^{(l)} Q_1^{(l)} Q_1^{(n)*} Q_k^{(n)*} \right], \quad (\text{A3})$$

$$m_{k,R}^z = \varepsilon_R \mu_R \sum_{l,n=1}^N \operatorname{Re} \left[\frac{1}{2i(\lambda^{(l)} - \lambda^{(n)*})} Q_k^{(l)} Q_N^{(l)} Q_N^{(n)*} Q_k^{(n)*} \right], \quad (\text{A4})$$

$$j_{k,k+1,L} = 2J\varepsilon_L \mu_L \sum_{l,n=1}^N \operatorname{Im} \left[\frac{1}{2i(\lambda^{(l)} - \lambda^{(n)*})} Q_k^{(l)} Q_1^{(l)} Q_1^{(n)*} Q_{k+1}^{(n)*} \right], \quad (\text{A5})$$

$$j_{k,k+1,R} = 2J\varepsilon_R \mu_R \sum_{l,n=1}^N \operatorname{Im} \left[\frac{1}{2i(\lambda^{(l)} - \lambda^{(n)*})} Q_k^{(l)} Q_N^{(l)} Q_N^{(n)*} Q_{k+1}^{(n)*} \right]. \quad (\text{A6})$$

Defining $[\mathbf{R}_l]_{m,n} \equiv Q_m^{(l)} Q_n^{(l)}$, and using eigenvalues and eigenvectors (22,23), magnetization on site k is obtained as

$$m_{k,L}^z = \begin{cases} \frac{l\mu_L}{l+r} \operatorname{Re} \left[\sum_q \frac{U_{N-k} \left(\frac{\tilde{\lambda}_q^*}{2} \right) + irU_{N-k-1} \left(\frac{\tilde{\lambda}_q^*}{2} \right)}{U_{N-1} \left(\frac{\tilde{\lambda}_q^*}{2} \right)} [\mathbf{R}_q^*]_{1,k} \right], & (k = 1 \sim N-1), \\ \frac{l\mu_L}{(l+r)(1+lr)}, & (k = N), \end{cases} \quad (\text{A7})$$

$$m_{k,R}^z = \begin{cases} \frac{r\mu_R}{(l+r)(1+lr)}, & (k = 1), \\ \frac{r\mu_R}{l+r} \operatorname{Re} \left[\sum_q \frac{U_{k-1} \left(\frac{\tilde{\lambda}_q^*}{2} \right) + ilU_{k-2} \left(\frac{\tilde{\lambda}_q^*}{2} \right)}{U_{N-1} \left(\frac{\tilde{\lambda}_q^*}{2} \right)} [\mathbf{R}_q^*]_{N,k} \right], & (k = 2 \sim N), \end{cases} \quad (\text{A8})$$

and spin current between sites k and $k+1$ is obtained as

$$j_{k,k+1,L}^z = \frac{2Jl\mu_L}{l+r} \operatorname{Im} \left[\sum_q \frac{U_{N-k} \left(\frac{\tilde{\lambda}_q^*}{2} \right) + irU_{N-k-1} \left(\frac{\tilde{\lambda}_q^*}{2} \right)}{U_{N-1} \left(\frac{\tilde{\lambda}_q^*}{2} \right)} [\mathbf{R}_q^*]_{1,k+1} \right], \quad (\text{A9})$$

$$j_{k,k+1,R}^z = \begin{cases} -\frac{2Jlr\mu_R}{(l+r)(1+lr)}, & (k = 1), \\ \frac{2Jr\mu_R}{l+r} \operatorname{Im} \left[\sum_q \frac{U_{k-1} \left(\frac{\tilde{\lambda}_q^*}{2} \right) + ilU_{k-2} \left(\frac{\tilde{\lambda}_q^*}{2} \right)}{U_{N-1} \left(\frac{\tilde{\lambda}_q^*}{2} \right)} [\mathbf{R}_q^*]_{N,k+1} \right], & (k = 2 \sim N), \end{cases} \quad (\text{A10})$$

where $U_k(x)$ is Chebyshev polynomial of the second kind for order k . Calculating these formulas, we derive the following Lemma.

Lemma 2. For the Hermitian conjugate of normalized matrix $\tilde{\Xi} \equiv (\Xi - B\mathbb{1})/J$, the component of $(k-m)$ -th power of the normalized matrix $\tilde{\Xi}$ is obtained as

$$\left[(\tilde{\Xi}^\dagger)^{k-m} \right]_{1,k} = \begin{cases} il, & (m = 0), \\ 1, & (m = 1), \\ 0, & (m = 2 \sim k). \end{cases} \quad (\text{A11})$$

This lemma can be proved easily. Since the normalized matrix $\tilde{\Xi}^\dagger$ has non-zero term at only secondary-diagonal part, the $(1,k)$ -component of $(k-m)$ -th power of the normalized matrix $\tilde{\Xi}$ is

$$\left[(\tilde{\Xi}^\dagger)^{k-m} \right]_{1,k} = \tilde{\Xi}_{1,m+1}^\dagger \tilde{\Xi}_{m+1,m+2}^\dagger \tilde{\Xi}_{m+2,m+3}^\dagger \cdots \tilde{\Xi}_{k-1,k}^\dagger. \quad (\text{A12})$$

For all $m(0 \leq m \leq k)$, the component $\tilde{\Xi}_{j,j+1}^\dagger$ is equal to 1, so the component $\left[\left(\tilde{\Xi}^\dagger\right)^{k-m}\right]_{1,k}$ is equal to $\tilde{\Xi}_{1,m+1}^\dagger$. Therefore, the component $\left[\left(\tilde{\Xi}^\dagger\right)^{k-m}\right]_{1,k}$ is classified by $\tilde{\Xi}_{1,m+1}^\dagger$. \square

By this lemma, magnetization and spin current for steady state is simplified. By using the recurrence relation for Chebyshev polynomial of the second kind $U_{n+1}(x) = 2xU_n(x) - U_{n-1}(x)$, the numerators in (A7-A10) is calculated as

$$U_{N-k} + irU_{N-k-1} = \left\{ \frac{ir}{1+rl} (\tilde{\lambda}_q^*)^k + \frac{1+r(r+l)}{1+rl} (\tilde{\lambda}_q^*)^{k-1} + \mathcal{O}((\tilde{\lambda}_q^*)^{k-2}) \right\} U_{N-1}, \quad (\text{A13})$$

$$(U_{k-1} + ilU_{k-2})(U_{N-1} - ilU_{N-2}) = \left(-\frac{il}{1+rl} (\tilde{\lambda}_q^*)^k + \frac{1}{1+rl} (\tilde{\lambda}_q^*)^{k-1} + \mathcal{O}((\tilde{\lambda}_q^*)^{k-2}) \right) U_{N-1}. \quad (\text{A14})$$

Substituting (A13,A14) to (A7-A10),

$$m_{k,L}^z = \begin{cases} \frac{l\mu_L}{l+r} \text{Re} \left[\frac{ir}{1+rl} (\tilde{\Xi}^\dagger)^k + \frac{1+r(r+l)}{1+rl} (\tilde{\Xi}^\dagger)^{k-1} + \mathcal{O}((\tilde{\Xi}^\dagger)^{k-2}) \right]_{1,k}, & (k = 1 \sim N-1), \\ \frac{l\mu_L}{(l+r)(1+lr)}, & (k = N), \end{cases} \quad (\text{A15})$$

$$m_{k,R}^z = \begin{cases} \frac{r\mu_R}{(l+r)(1+lr)}, & (k = 1), \\ \frac{r\mu_R}{l+r} \text{Re} \left[-\frac{il}{1+rl} (\tilde{\Xi}^\dagger)^k + \frac{1}{1+rl} (\tilde{\Xi}^\dagger)^{k-1} + \mathcal{O}((\tilde{\Xi}^\dagger)^{k-2}) \right]_{1,k}, & (k = 2 \sim N), \end{cases} \quad (\text{A16})$$

$$j_{k,k+1,L}^z = \frac{2Jl\mu_L}{l+r} \text{Im} \left[\frac{ir}{1+rl} (\tilde{\Xi}^\dagger)^k + \frac{1+r(r+l)}{1+rl} (\tilde{\Xi}^\dagger)^{k-1} + \mathcal{O}((\tilde{\Xi}^\dagger)^{k-2}) \right]_{1,k+1}, \quad (\text{A17})$$

$$j_{k,k+1,R}^z = \begin{cases} -\frac{2Jlr\mu_R}{(l+r)(1+lr)}, & (k = 1), \\ \frac{2Jr\mu_R}{l+r} \text{Im} \left[-\frac{il}{1+rl} (\tilde{\Xi}^\dagger)^k + \frac{1}{1+rl} (\tilde{\Xi}^\dagger)^{k-1} + \mathcal{O}((\tilde{\Xi}^\dagger)^{k-2}) \right]_{1,k+1}, & (k = 2 \sim N). \end{cases} \quad (\text{A18})$$

Applying lemma to the above formulas,

$$m_k^z = \mu_L - bD_k^{(L)} = \mu_R + bD_k^{(R)}, \quad j = \frac{2Jlr(\mu_L - \mu_R)}{(1+lr)(l+r)}, \quad (\text{A19})$$

where $l = \varepsilon_L/4J, r = \varepsilon_R/4J$ and $j = 2b$. The sequences $D^{L/R}$ are defined as

$$D_k^{(L)} = \{l^{-1}, l+l^{-1}, \dots, l+l^{-1}, l+l^{-1}+r\}, \quad (\text{A20})$$

$$D_k^{(R)} = \{r+r^{-1}+l, r+r^{-1}, \dots, r+r^{-1}, r^{-1}\}. \quad (\text{A21})$$

Appendix B: Calculation of time derivative of magnetization

We start the calculation of the time derivative of magnetization $\mu_k(t)$ from (60). The summations in (60) include the terms for the special eigenstates and the term for the normal eigenstates, and is separated as

$$\sum_{l=1}^N e^{-2t\beta_l} Q_n^{(l)} Q_m^{(l)} = \sum_{l \in \ell'} e^{-2t\beta_l} Q_n^{(l)} Q_m^{(l)} + \sum_{l \in \{\text{sp}\}} e^{-2t\beta_l} Q_n^{(l)} Q_m^{(l)}, \quad (\text{B1})$$

where $\ell' \in \{1, 2, \dots, N\} \setminus \{\text{sp}\}$. The first term in (B1) is the part of the normal eigenstates, and the second one is the part of the special eigenstates. At first, we calculate the part of the normal eigenstates. For large N , normalization factor \mathcal{N}_l for the normal eigenstate can be calculated by using the component of the l -th eigenvector corresponding to a normal eigenvalue (23) as

$$\mathcal{N}_l^2 \approx \frac{N}{2 \sin^2 \theta_l} \left(1 + \frac{i\varepsilon_L}{2J} \cos \theta_l + \frac{\varepsilon_L^2}{16J^2} \right), \quad (\text{B2})$$

and eigenvalues of matrix \mathbf{X} are $\beta_l = i\lambda^{(l)} = 2iJ \cos \frac{l}{N+1}\pi + \mathcal{O}(N^{-2})$. Then, the summation

$$\sum_{l \in \ell'} e^{-2t\beta_l} Q_n^{(l)} Q_m^{(l)} \approx \frac{2}{\pi} \int_0^\pi \frac{e^{-4iJt \cos x}}{1 + \frac{i\varepsilon_L}{2J} \cos x - \frac{\varepsilon_L^2}{16J^2}} \left(\sin nx + \frac{i\varepsilon_L}{4J} \sin(n-1)x \right) \left(\sin mx + \frac{i\varepsilon_L}{4J} \sin(m-1)x \right) dx. \quad (\text{B3})$$

The exponential in integrated function for above equation (B3) is transformed as

$$\frac{e^{-4iJt \cos x}}{1 + \frac{i\varepsilon_L}{2J} \cos x - \frac{\varepsilon_L^2}{16J^2}} = \begin{cases} \frac{8J^2}{\varepsilon_L} \int_t^\infty e^{-4iJs \cos x} e^{-2J\left(\frac{\varepsilon_L}{4J} - \frac{4J}{\varepsilon_L}\right)(t-s)} ds, & \left(\frac{\varepsilon_L}{4J} < 1\right), \\ -\frac{8J^2}{\varepsilon_L} \int_{-\infty}^t e^{-4iJs \cos x} e^{-2J\left(\frac{\varepsilon_L}{4J} - \frac{4J}{\varepsilon_L}\right)(t-s)} ds, & \left(\frac{\varepsilon_L}{4J} > 1\right). \end{cases} \quad (\text{B4})$$

Using the integral form of the Bessel function of n th order

$$J_n(z) = \frac{i^n}{\pi} \int_0^\pi e^{-iz \cos \theta} \cos n\theta d\theta, \quad (\text{B5})$$

we can calculate (B3) when $\varepsilon_L < 4J$

$$\sum_{l \in \ell'} e^{-2t\beta_l} Q_n^{(l)} Q_m^{(l)} \approx i^{-n-m} \frac{8J^2}{\varepsilon_L} \int_t^\infty ds e^{-2J\left(\frac{\varepsilon_L}{4J} - \frac{4J}{\varepsilon_L}\right)(t-s)} Y_{n,m}(4Js), \quad (\text{B6})$$

where we define the function $Y_{n,m}(t)$ as

$$Y_{n,m}(t) = (-1)^m J_{n-m}(t) - J_{n+m}(t) + \frac{\varepsilon_L}{4J} (2J_{n+m-1}(t) + (-1)^m J_{n-m+1}(t) - (-1)^m J_{n-m-1}(t)) - \frac{\varepsilon_L^2}{16J^2} (J_{n+m-2}(t) + (-1)^m J_{n-m}(t)). \quad (\text{B7})$$

We can calculate the $\varepsilon_L > 4J$ case by a similar procedure.

We can also calculate the $\varepsilon_L = 4J$ case using a slightly different procedure. When $\varepsilon_L = 4J$, (B3) is calculated as

$$\sum_{l \in \ell'} e^{-2t\beta_l} Q_n^{(l)} Q_m^{(l)} \approx \frac{2}{\pi} \int_0^\pi \frac{e^{-4iJt \cos x}}{2i \cos x} (\sin nx + i \sin(n-1)x) (\sin mx + i \sin(m-1)x) dx. \quad (\text{B8})$$

The exponential in the integrated function for above equation (B8) is transformed as

$$\frac{e^{-4iJt \cos x}}{2i \cos x} = -2J \left(\int_0^t e^{-4iJs \cos x} ds + \frac{1}{-4iJ \cos x} \right). \quad (\text{B9})$$

Using the integral form of the Bessel function of n th order, we can calculate (B8)

$$\begin{aligned} \sum_{l \in \ell'} e^{-2t\beta_l} Q_n^{(l)} Q_m^{(l)} &\approx -2J i^{-n-m} \int_0^t Y_{n,m}(4Js) ds \\ &+ \frac{1}{\pi i} \int_0^\pi \frac{(\sin nx + i \sin(n-1)x) (\sin mx + i \sin(m-1)x)}{\cos x} dx \end{aligned} \quad (\text{B10})$$

Using the lemma for integrations using the Chebyshev polynomial[73] as the follows,

$$\int_{-1}^1 \frac{T_n(x)}{(x-y)\sqrt{1-x^2}} dx = \pi U_{n-1}(y), \quad \int_{-1}^1 \frac{\sqrt{1-x^2} U_{n-1}(x)}{x-y} dx = -\pi T_n(y), \quad (\text{B11})$$

and the lemma for integration using the Bessel function[72] as the follows,

$$\int_0^\infty J_\nu(t) dt = 1, \quad (\text{Re}\{\nu\} > -1), \quad (\text{B12})$$

we obtain the following form when $\varepsilon_L = 4J$,

$$\sum_{l \in \ell'} e^{-2t\beta_l} Q_n^{(l)} Q_m^{(l)} \approx i^{-n-m} \left(2J \int_t^\infty Y_{n,m}(4Js) ds + (-1)^{n+m} - (-1)^n \delta_{n,m} \right). \quad (\text{B13})$$

Thus, the formula (B13) when $\varepsilon_L = 4J$ takes the formula of adding the static term for time t to the formula (B6) when $\varepsilon_L < 4J$.

Next, we calculate the part of the special eigenstates. In this paper, we obtain the formula of special eigenvalue for infinite and finite system size (22,27). For large N , we define $\theta_{\text{sp}} = x_{\text{sp}} + iy_{\text{sp}}$. Since $\cos \theta_{\text{sp}}$ is a pure imaginary, i.e., $\cos \theta_{\text{sp}} \in i\mathbb{R}$, we determine $x_{\text{sp}} = \pm \frac{\pi}{2}$, and we consider $x_{\text{sp}} = \frac{\pi}{2}$. Then, we can calculate $y_{\text{sp}} = \log(\frac{\varepsilon_L/R}{4J})$. Then, we can calculate $\sin k\theta_{\text{sp}} = \frac{1}{2i} \left(\left(-\frac{i\varepsilon_L/R}{4J} \right)^{-k} - \left(-\frac{i\varepsilon_L/R}{4J} \right)^k \right)$, and normalized factor \mathcal{N}_{sp} is

$$\mathcal{N}_{\text{sp}}^2 \approx \begin{cases} \left(1 + \left(\frac{\varepsilon_L}{4J} \right)^{-2} \right)^{-1} & \left(\frac{\varepsilon_L}{4J} > 1 \right), \\ \frac{\left(\frac{\varepsilon_R}{4J} - \frac{\varepsilon_L}{4J} \right)^2 \left(-i\frac{\varepsilon_R}{4J} \right)^{2N+2}}{\left(1 + \left(\frac{\varepsilon_R}{4J} \right)^2 \right)^3} & \left(\frac{\varepsilon_R}{4J} > 1 \right). \end{cases} \quad (\text{B14})$$

The leading term for the part of the special eigenstates is calculated as

$$e^{-2t\lambda_{\text{sp}}} Q_n^{(\text{sp})} Q_m^{(\text{sp})} \approx \begin{cases} -e^{-2J\left(\frac{\varepsilon_L}{4J} - \frac{4J}{\varepsilon_L}\right)t} \left(1 + \left(\frac{\varepsilon_L}{4J} \right)^2 \right) \left(-\frac{i\varepsilon_L}{4J} \right)^{-n-m} & \left(\frac{\varepsilon_L}{4J} > 1 \right), \\ -e^{-2J\left(\frac{\varepsilon_R}{4J} - \frac{4J}{\varepsilon_R}\right)t} \left(1 + \left(\frac{\varepsilon_R}{4J} \right)^2 \right) \left(-\frac{i\varepsilon_R}{4J} \right)^{-2N-2+n+m} & \left(\frac{\varepsilon_R}{4J} > 1 \right). \end{cases} \quad (\text{B15})$$

Then, we can obtain the formulas (61).

-
- [1] F. Bonetto, J. Lebowitz, and L. Rey-Bellet, arXiv:math-ph/0002052 (2000).
 - [2] A. Sone, Y.-X. Liu, and P. Cappellaro, Phys. Rev. Lett. **125**, 060602 (2020).
 - [3] S. Chandrasekhar, *Hydrodynamic and hydromagnetic stability* (Oxford Univ. Press, 1961).
 - [4] E. L. Koschmieder, *Bénard cells and Taylor vortices* (Cambridge University Press, 1993).
 - [5] A. V. Getling, *Rayleigh-Bénard Convection: Structures and Dynamics*, Vol. 11 (World Scientific, 1998).
 - [6] B. Derrida, J. Stat. Mech. **2007**, P07023 (2007).
 - [7] A. Dhar, Adv. Phys. **57**, 457 (2008).
 - [8] H. Spohn, J. Stat. Phys. **154**, 1191 (2014).
 - [9] S. Diehl, A. Micheli, A. Kantian, B. Kraus, H. Büchler, and P. Zoller, Nature **4**, 878 (2008).
 - [10] N. Syassen, D. M. Bauer, M. Lettner, T. Volz, D. Dietze, J. J. Garcia-Ripoll, J. I. Cirac, G. Rempe, and S. Dürr, Science **320**, 1329 (2008).
 - [11] M. Cheneau, P. Barmettler, D. Poletti, M. Endres, P. Schauß, T. Fukuhara, C. Gross, I. Bloch, C. Kollath, and S. Kuhr, Nature **481**, 484 (2012).
 - [12] T. Tomita, S. Nakajima, I. Danshita, Y. Takasu, and Y. Takahashi, Sci. adv. **3**, e1701513 (2017).
 - [13] P. Nation, J. Johansson, M. Blencowe, and A. Rimberg, Phys. Rev. E **91**, 013307 (2015).
 - [14] P. Nation, arXiv:1504.06768 (2015).
 - [15] L. Xiao, X. Zhan, Z. Bian, K. Wang, X. Zhang, X. Wang, J. Li, K. Mochizuki, D. Kim, N. Kawakami, *et al.*, Nature Physics **13**, 1117 (2017).
 - [16] M. van Caspel, S. E. T. Arze, and I. P. Castillo, SciPost Phys. **6**, 26 (2019).
 - [17] N. Shibata and H. Katsura, Phys. Rev. B **99**, 174303 (2019).
 - [18] N. Shibata and H. Katsura, Phys. Rev. B **99**, 224432 (2019).
 - [19] J. Huber, P. Kirton, S. Rotter, and P. Rabl, arXiv:2003.02265 (2020).
 - [20] J. Huber, P. Kirton, and P. Rabl, Phys. Rev. A **102**, 012219 (2020).
 - [21] J. Schwinger, J. Math. Phys. **2**, 407 (1961).
 - [22] L. V. Keldysh *et al.*, Sov. Phys. JETP **20**, 1018 (1965).
 - [23] L. P. Kadanoff and G. A. Baym, *Quantum Statistical Mechanics* (Benjamin, New York, 1962).
 - [24] M. Cini, Phys. Rev. B **22**, 5887 (1980).
 - [25] G. Stefanucci and C.-O. Almbladh, Phys. Rev. B **69**, 195318 (2004).
 - [26] P. Myöhänen, A. Stan, G. Stefanucci, and R. van Leeuwen, Phys. Rev. B **80**, 115107 (2009).
 - [27] M. Ridley, A. MacKinnon, and L. Kantorovich, Phys. Rev. B **91**, 125433 (2015).
 - [28] T. Fukadai and T. Sasamoto, arXiv:1912.05633 (2019).
 - [29] A. G. Redfield, IBM Journal of Research and Development **1**, 19 (1957).
 - [30] G. Lindblad, Commun. Math. Phys. **48**, 119 (1976).
 - [31] H.-P. Breuer and F. Petruccione, *The Theory of Open Quantum Systems* (Oxford Univ. Press, 2002).
 - [32] M. Žnidarič, J. Stat. Mech. , L05002 (2010).
 - [33] M. Žnidarič, J. Phys. A **43**, 415004 (2010).

- [34] M. Žnidarič, Phys. Rev. E **83**, 011108 (2011).
- [35] T. Prosen, Phys. Rev. Lett. **106**, 217206 (2011).
- [36] T. Prosen, Phys. Rev. Lett. **107**, 137201 (2011).
- [37] D. Karevski, V. Popkov, and G. M. Schütz, Phys. Rev. Lett. **110**, 047201 (2013).
- [38] T. Prosen, J. Phys. A **48**, 373001 (2015).
- [39] C. Matsui and T. Prosen, J. Phys. A **50**, 385201 (2017).
- [40] P. Ribeiro and T. Prosen, Phys. Rev. Lett. **122**, 010401 (2019).
- [41] S. Clark, J. Prior, M. Hartmann, D. Jaksch, and M. B. Plenio, New J. Phys. **12**, 025005 (2010).
- [42] D. Muth, R. G. Unanyan, and M. Fleischhauer, Phys. Rev. Lett. **106**, 077202 (2011).
- [43] M. P. Zaletel, R. S. Mong, C. Karrasch, J. E. Moore, and F. Pollmann, Phys. Rev. B **91**, 165112 (2015).
- [44] U. Schollwöck, Rev. Mod. Phys. **77**, 259 (2005).
- [45] T. Prosen and M. Žnidarič, J. Stat. Mech. **2009**, P02035 (2009).
- [46] T. Prosen, New J. Phys. **10**, 043026 (2008).
- [47] T. Prosen and I. Pižorn, Phys. Rev. Lett. **101**, 105701 (2008).
- [48] T. Prosen and B. Žunkovič, New J. Phys. **12**, 025016 (2010).
- [49] T. Prosen, J. Stat. Mech. , P07020 (2010).
- [50] T. Prosen and T. H. Seligman, J. Phys. A **43**, 392004 (2010).
- [51] C. Guo and D. Poletti, Phys. Rev. A **95**, 052107 (2017).
- [52] C. Guo and D. Poletti, Phys. Rev. A **98**, 052126 (2018).
- [53] H. Abou-Kandil, G. Freiling, V. Ionescu, and G. Jank, *Matrix Riccati Equations in Control and Systems Theory* (Springer Basel AG, 2003).
- [54] J. M. Davis, I. A. Gravagne, J. R. Marks II, and A. A. Ramos, arXiv:0910.1895 (2009).
- [55] M. Behr, P. Benner, and J. Heiland, Calcolo **56** (2019).
- [56] W. Liu and N. Andrei, Phys. Rev. Lett. **112**, 257204 (2014).
- [57] K. Najafi, M. Rajabpour, and J. Viti, Phys. Rev. B **97**, 205103 (2018).
- [58] F. L. Rodrigues, G. De Chiara, M. Paternostro, and G. T. Landi, Phys. Rev. Lett. **123**, 140601 (2019).
- [59] L. H. Reis, S. H. Silva, and E. Pereira, Phys. Rev. E **101**, 062107 (2020).
- [60] W. Yueh, Applied Mathematics E-Notes **5**, 66 (2005).
- [61] R. Witula and D. Ślota, J. Math. Anal. Appl. **324**, 321 (2006).
- [62] B. Žunkovič and T. Prosen, J. Stat. Mech. , P08016 (2010).
- [63] S. Ajisaka, F. Barra, and B. Žunkovič, New J. Phys. **16**, 033028 (2014).
- [64] M. Žnidarič, B. Žunkovič, and T. Prosen, Phys. Rev. E **84**, 051115 (2011).
- [65] L. C. Venuti and P. Zanardi, Phys. Rev. A **93**, 032101 (2016).
- [66] *Foundations of Optimal Control Theory* (John Wiley & Sons, 1967).
- [67] *Foundations of Optimal Control Theory* (Prentice-Hall, 1970).
- [68] S. Mondié, A. V. Egorov, and M. A. Gomez, IFAC-PapersOnLine **51**, 136 (2018).
- [69] E. H. Lieb and D. W. Robinson, Commun. Math. Phys. **28**, 251 (1972).
- [70] W. Liu, *Time evolution of the XXZ Heisenberg model*, Ph.D. thesis, Rutgers, The State University of New Jersey (2014).
- [71] I. Pižorn and T. Prosen, Phys. Rev. B **79**, 184416 (2009).
- [72] M. Abramowitz and I. A. Stegun, *Handbook of mathematical functions with formulas, graphs, and mathematical tables*, Vol. 55 (US Government printing office, 1948).
- [73] J. C. Mason and D. C. Handscomb, *Chebyshev polynomials* (CRC press, 2002).